

# 000 001 002 003 004 005 006 007 008 009 010 011 012 013 014 015 016 017 018 019 020 021 022 023 024 025 026 027 028 029 030 031 032 033 034 035 036 037 038 039 040 041 042 043 044 045 046 047 048 049 050 051 052 053 CONFORMAL ROBUSTNESS CONTROL: A NEW STRATEGY FOR ROBUST DECISION

Anonymous authors

Paper under double-blind review

## ABSTRACT

Robust decision-making is crucial in numerous risk-sensitive applications where outcomes are uncertain and the cost of failure is high. [Conditional Robust Optimization \(CRO\)](#) offers a framework for such tasks by constructing prediction sets for the outcome that satisfy predefined coverage requirements and then making decisions based on these sets. Many existing approaches leverage conformal prediction to build prediction sets with guaranteed coverage for CRO. However, since coverage is a *sufficient but not necessary* condition for robustness, enforcing such constraints often leads to overly conservative decisions. To overcome this limitation, we propose a novel framework named Conformal Robustness Control (CRC), that directly optimizes the prediction set construction under explicit robustness constraints, thereby enabling more efficient decisions without compromising robustness. We develop efficient algorithms to solve the CRC optimization problem, and also provide theoretical guarantees on both robustness and optimality. Empirical results show that CRC consistently yields more effective decisions than existing baselines while still meeting the target robustness level.

## 1 INTRODUCTION

In many real-world applications, it is crucial for decision-makers to account for operational risks to avoid irreversible consequences. For example, portfolio management (Markowitz, 1952) aims to maximize returns while navigating the trade-off with risk tolerance. Similar risk-sensitive decision-making challenges are also evident in fields such as medical diagnosis (Kiyani et al., 2025) and transportation planning (Patel et al., 2024).

Consider a scenario where we observe an input  $X$ , but the corresponding outcome  $Y$  is unknown. The decision-maker needs to choose a decision  $z(X)$  based on the input  $X$  such that the incurred decision loss  $\phi(Y, z(X))$  does not exceed a certain *risk certificate*  $r(X)$  with high probability. Formally, the  $(1 - \alpha)$ -level robustness requirement is given by

$$\mathbb{P}\{\phi(Y, z(X)) \leq r(X)\} \geq 1 - \alpha. \quad (1)$$

At the same time, the decision-maker seeks to minimize  $r(X)$  to improve efficiency and reduce potential worst-case losses.

Over the years, Conditional Robust Optimization (CRO), introduced by Chenreddy et al. (2022), has become a widely adopted and effective framework for robust decision-making. As an extension of classical robust optimization (Ben-Tal et al., 2009), CRO incorporates covariate information to enhance decision quality, enabling more precise and context-aware responses in complex tasks. In the CRO framework, decisions are derived from a minmax optimization problem using a prediction set  $\mathcal{U}(X)$ , formulated as  $z_{\mathcal{U}}(X) := \arg \min_{z \in \mathcal{Z}} \max_{y \in \mathcal{U}(X)} \phi(y, z)$ . By designing  $\mathcal{U}(X)$  with a regular structure, such as a box or an ellipse, the resulting minmax problem remains convex and can be solved efficiently in polynomial time. The corresponding risk certificate value is defined as  $r_{\mathcal{U}}(X) := \max_{y \in \mathcal{U}(X)} \phi(y, z_{\mathcal{U}}(X))$ . To meet the robustness requirement (1), CRO enforces a coverage condition on the prediction set, that is

$$\mathbb{P}\{Y \in \mathcal{U}(X)\} \geq 1 - \alpha. \quad (2)$$

Recently, Johnstone & Cox (2021) and Sun et al. (2023) first employed the conformal prediction (Vovk et al., 2005) to construct the prediction set  $\mathcal{U}(X)$  from historical labeled data with the target

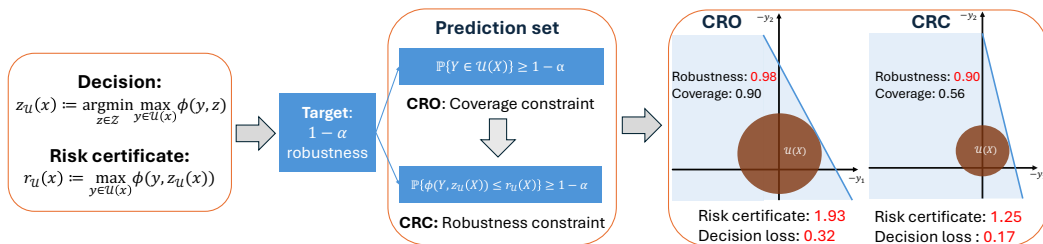
054 coverage level  $1 - \alpha$ ; then substituted it into the minmax problem to make the final decision. It can  
 055 be observed that the coverage property (2) is a sufficient condition for achieving the final robustness  
 056 target (1). Hence, the two-step procedure above provides a statistically valid robustness guarantee  
 057 for the subsequent decisions.

058 However, as noted by Ben-Tal et al. (2009), controlling robustness via this sufficient condition often  
 059 results in suboptimal and overly conservative decisions. In this paper, we introduce Conformal  
 060 Robustness Control (CRC), a new strategy to alleviate the conservativeness of the existing CRO  
 061 framework and to enable more efficient robust decisions. Our contributions are summarized as  
 062 follows.

063

- (1) Unlike conventional CRO methods that enforce coverage constraint on prediction sets,  
 064 CRC directly minimizes the expected risk certificate under explicit robustness constraint,  
 065 significantly improving decision efficiency. The CRC procedure is amenable to efficient  
 066 gradient-based optimization algorithms that minimize an empirical loss using labeled data.
- (2) We establish non-asymptotic theoretical guarantees on both the robustness and the optimality  
 067 gap of the resulting decisions. For a given test data point, we further develop a  
 068 sample-splitting calibration procedure to endow the optimized prediction set with finite-  
 069 sample robustness guarantees.
- (3) Through extensive experiments on both synthetic data and real-world applications, the pro-  
 070 posed CRC consistently outperforms baseline methods across key metrics.

071  
 072 Figure 1 compares the conventional CRO framework with our proposed method CRC, at the nominal  
 073 robustness level  $1 - \alpha = 90\%$ . The brown circular regions in the right panel represent prediction  
 074 sets  $\mathcal{U}(X)$  satisfying a 90% coverage constraint and a 90% robustness constraint, respectively. The  
 075 CRO decision attains a robustness level of 98%, which is significantly higher than the nominal  
 076 requirement. This leads to a higher risk certificate and decision loss compared to the proposed CRC.



077  
 078 Figure 1: Comparison of CRO and our method CRC. Portfolio optimization problem with  
 079 with  $\phi(y, z) = -y^\top z$ ,  $\mathcal{Z} = \{z \in \mathbb{R}^2 : z_1 + z_2 = 1, z_1, z_2 \geq 0\}$ , and  $\alpha = 0.1$ . Blue lines show  
 080 CRO solutions for the brown circular prediction sets. The shaded blue regions indicate where the  
 081 loss  $\phi(y, z(X))$  is below the risk certificate  $r(X)$ . The prediction set in CRO achieves exact 90%  
 082 coverage, with  $r(X) = 1.93$ . In contrast, CRC meets the 90% robustness requirement, yielding a  
 083 more efficient decision with  $r(X) = 1.25$ .

## 2 RELATED WORKS

094 Robust optimization is a well-established method for decision-making under uncertainty. Early  
 095 work focused on approximating Value at Risk (VaR) by designing deterministic prediction sets to  
 096 induce robustness (Ghaoui et al., 2003; Natarajan et al., 2008; Bertsimas et al., 2018). Later studies,  
 097 such as Shang et al. (2017); Bertsimas et al. (2018); Hong et al. (2021), have proposed data-driven  
 098 prediction sets. With the growing size of data, Chenreddy et al. (2022) explored how covariate in-  
 099 formation could be leveraged to develop more effective prediction sets, leading to the introduction  
 100 of the Conformal Robust Optimization (CRO) framework. Subsequent works by Johnstone & Cox  
 101 (2021); Patel et al. (2024); Sun et al. (2023) incorporated conformal prediction methods to construct  
 102 prediction sets that satisfy coverage conditions, thereby providing finite-sample robustness guar-  
 103 antees for CRO. Kiyani et al. (2025) derived the explicit form of the optimal prediction set that has the  
 104

minimum risk certificate under the coverage constraint. However, the construction relies on minimizing the VaR function, which often also leads to intractable formulations if the decision space is continuous (Uryasev & Rockafellar, 2001). In addition, Wang et al. (2023) also considered optimizing the prediction sets in a robust optimization problem, but relaxing the robustness constraint through the conditional Value at Risk transformation (Rockafellar & Uryasev, 2002). Compared to existing work, we impose the exact robustness constraint rather than a coverage constraint on the prediction set, thereby enhancing the generation of more effective decisions.

Conformal prediction is a widely used method for uncertainty quantification, notable for its model-agnostic and distribution-free properties (Vovk et al., 2005; Lei et al., 2018; Angelopoulos et al., 2024a). In predictive inference tasks, the efficiency measure of conformal prediction sets is the size or volume. Recent research has increasingly focused on improving the efficiency of these prediction sets. Several studies, such as Sadinle et al. (2019), Bai et al. (2022), Stutz et al. (2022), and Kiyani et al. (2024b) have formulated constrained optimization problems that minimize the size of prediction sets subject to coverage constraints. In addition, Yang & Kuchibhotla (2025) introduced a sample-splitting approach to select models yielding the smallest prediction sets, followed by constructing split conformal prediction sets (Vovk et al., 2005; Papadopoulos et al., 2002). Differently, Liang et al. (2024) proposed a method that avoids sample splitting while maintaining finite-sample coverage during model selection. In terms of decision efficiency, since the performance of decisions varies significantly with different conformal prediction sets, Chenreddy & Delage (2024) and Yeh et al. (2024) proposed end-to-end learning methods that train the conformal prediction sets by directly minimizing downstream expected decision risk. Moreover, Bao et al. (2025) developed new frameworks for prediction set selection in the CRO problem, which could keep finite-sample robustness control while avoiding sample splitting.

### 3 PREDICTION SET OPTIMIZATION WITH ROBUSTNESS CONTROL

#### 3.1 PROBLEM SETUP

Let  $\mathcal{X}$  be the covariate space, and  $\mathcal{Y}$  be the label space. The primary goal of robust decision is to find a decision policy  $z(\cdot) : \mathcal{X} \rightarrow \mathcal{Z}$  and a risk certificate function  $r(\cdot) : \mathcal{X} \rightarrow \mathbb{R}$  that minimizes  $\mathbb{E}[r(X)]$  subject to the robustness constraint in (1). [It is consistent with the Risk Averse Decision Policy Optimization \(RA-DPO\) problem defined by Kiyani et al. \(2025\):](#)

$$\min_{z(\cdot), r(\cdot)} \mathbb{E}[r(X)] \quad \text{s.t.} \quad \mathbb{P}\{\phi(Y, z(X)) \leq r(X)\} \geq 1 - \alpha. \quad (3)$$

However, directly optimizing over arbitrary forms of  $z(\cdot)$  and  $r(\cdot)$  is generally difficult. The CRO framework provides a flexible alternative by introducing a prediction set  $\mathcal{U}(\cdot)$  that maps each covariate  $x \in \mathcal{X}$  to a subset of the label space  $\mathcal{Y}$ , which relates to both the decision and the associated risk certificate. Specifically, for  $x \in \mathcal{X}$ ,

$$z_{\mathcal{U}}(x) := \arg \min_{z \in \mathcal{Z}} \max_{y \in \mathcal{U}(x)} \phi(y, z), \quad r_{\mathcal{U}}(x) = \max_{y \in \mathcal{U}(x)} \phi(y, z_{\mathcal{U}}(x)).$$

To identify the optimal decision policy and risk certificate, it is natural to minimize the expected risk certificate under the robustness constraint:

$$\min_{\mathcal{U}(\cdot) : \mathcal{X} \rightarrow 2^{\mathcal{Y}}} \mathbb{E}[r_{\mathcal{U}}(X)] \quad \text{s.t.} \quad \mathbb{P}\{\phi(Y, z_{\mathcal{U}}(X)) \leq r_{\mathcal{U}}(X)\} \geq 1 - \alpha. \quad (4)$$

The next theorem shows the equivalence between RA-DPO in (3) and the problem (4), which also means that optimizing the prediction sets will not result in a suboptimal risk certificate.

**Theorem 3.1.** *Let  $z^{RA\text{-DPO}}(\cdot), r^{RA\text{-DPO}}(\cdot)$  be the optimal solution of RA-DPO in (3), and let  $\mathcal{U}^*$  be the optimal solution of (4). It holds that  $\mathbb{E}[r^{RA\text{-DPO}}(X)] = \mathbb{E}[r_{\mathcal{U}^*}(X)]$ , which means problems (3) and (4) are equivalent in minimizing the expected risk certificate while maintaining robustness control.*

We defer the proof of Theorem 3.1 to Appendix B.2. The prior work of Kiyani et al. (2025) also derived a formulation equivalent to RA-DPO in Eq. (3), termed Risk Averse Conformal Prediction Optimization (RA-CPO). This formulation optimizes the expected risk certificate over all possible prediction sets subject to a coverage constraint, that is, replacing the constraint in (4) with (2). To construct the “optimal” prediction set that solves RA-CPO, Kiyani et al. (2025)

proposed a method based on the minimizer and minimum value of a contextual VaR problem:  $z^*(x) = \arg \min_{z \in \mathcal{Z}} \text{VaR}_{1-\alpha}(\phi(Y, z) | X = x)$  and  $r^*(x) = \min_{z \in \mathcal{Z}} \text{VaR}_{1-\alpha}(\phi(Y, z) | X = x)$ . Here,  $\text{VaR}(\cdot | X = x)$  denotes the conditional  $1 - \alpha$  population quantile given the covariate  $X = x$ . In the case of classification with a finite decision space, Kiyani et al. (2024a) approximated the optimal prediction set by first estimating the conditional distribution of  $Y | X$ , then the associated VaR problem can be solved by traversal. However, this approach does not extend to continuous decision spaces  $\mathcal{Z}$ , where the VaR problem generally becomes intractable (Uryasev & Rockafellar, 2001).

To address this limit, we consider solving problem (4) over the parametrized prediction set  $\mathcal{U}_\theta(\cdot)$ , where  $\theta \in \Theta$  refers to the model parameters. In regression settings with  $\mathcal{X} = \mathbb{R}^p$ ,  $\mathcal{Y} = \mathbb{R}^q$ , two commonly used types of prediction sets are *box* and *ellipsoidal* sets (Johansson et al., 2017; Sun et al., 2023). Their parametrized forms are can be defined as follows.

- **Box prediction set.** A box-shaped prediction set is constructed by componentwise lower and upper bounds for the response vector. Let  $h_\theta^{\text{lo}}(\cdot) : \mathbb{R}^p \rightarrow \mathbb{R}^q$  and  $h_\theta^{\text{hi}}(\cdot) : \mathbb{R}^p \rightarrow \mathbb{R}^q$  be models with parameters  $\theta \in \Theta$ , then

$$\mathcal{U}_\theta(x) = \{y \in \mathbb{R}^q : h_\theta^{\text{lo}}(x) \leq y \leq h_\theta^{\text{hi}}(x)\}.$$

- **Ellipsoidal prediction set.** Unlike box sets, ellipsoidal prediction sets account for correlations among components of the response vector. Let  $\mu_\theta(\cdot) : \mathbb{R}^p \rightarrow \mathbb{R}^q$  and  $\Sigma_\theta(\cdot) : \mathbb{R}^p \rightarrow \mathbb{R}^{q \times q}$  denote the mean and covariance model with parameters  $\theta \in \Theta$ , then

$$\mathcal{U}_\theta(x) = \left\{y \in \mathbb{R}^q : (y - \mu_\theta(x))^\top \Sigma_\theta^{-1}(x) (y - \mu_\theta(x)) \leq 1\right\}.$$

In Appendix E.6, we also provide the example of a parametrized polyhedral set based on the definition in Bärmann et al. (2016).

For a parametrized prediction set  $\mathcal{U}_\theta(\cdot)$ , we denote the corresponding decision policy and risk certificate functions as  $z_\theta(\cdot) \equiv z_{\mathcal{U}_\theta}(\cdot)$  and  $r_\theta(\cdot) \equiv r_{\mathcal{U}_\theta}(\cdot)$  for short. We then consider the parameterized version of problem (4):

$$\min_{\theta \in \Theta} \mathbb{E}[r_\theta(X)] \quad \text{s.t.} \quad \mathbb{P}\{\phi(Y, z_\theta(X)) \leq r_\theta(X)\} \geq 1 - \alpha. \quad (5)$$

Even though the parametrized optimization can also be applied to the RA-CPO framework, we show that our proposed problem (5) yields a lower risk certificate in Appendix B.3, which further confirms the benefit of robustness constraint over the coverage constraint. In the following subsections, we investigate the optimization problem (5) based on the collected labeled data and provide theoretical results for the robustness and optimality guarantees. Moreover, we also developed a differential algorithm to solve the optimization problem for the continuous decision space.

### 3.2 EMPIRICAL OPTIMIZATION WITH CONFORMAL ROBUSTNESS CONTROL

Suppose we have collected an i.i.d. labeled dataset  $\mathcal{D}_n = \{(X_i, Y_i)\}_{i=1}^n$  drawn from some distribution  $P$ . We first optimize the prediction set by addressing an empirical version of the problem (5), and then apply this prediction set for decision-making. By approximating both the objective and the constraint in (5) via sample averaging, we obtain the following empirical counterpart:

$$\hat{\theta} = \arg \min_{\theta \in \Theta} \frac{1}{n} \sum_{i=1}^n r_\theta(X_i) \quad \text{s.t.} \quad \frac{1}{n} \sum_{i=1}^n \mathbb{1}\{\phi(Y_i, z_\theta(X_i)) \leq r_\theta(X_i)\} \geq 1 - \alpha. \quad (6)$$

To distinguish from coverage control methods and to emphasize the explicit robustness constraint, we refer to this procedure as *Conformal Robustness Control* (CRC).

A natural approach to solving problem (6) is to consider its dual formulation. Define the Lagrangian function as  $L(\lambda; \theta) := f(\theta) + \lambda g(\theta)$ , where  $\lambda \geq 0$  is the Lagrange multiplier,  $f(\theta) = \frac{1}{n} \sum_{i=1}^n r_\theta(X_i)$  and  $g(\theta) = 1 - \alpha - \frac{1}{n} \sum_{i=1}^n \mathbb{1}\{\phi(Y_i, z_\theta(X_i)) \leq r_\theta(X_i)\}$ . The function  $f(\theta)$  is typically differentiable if the CPO problem for  $\mathcal{U}_\theta(x)$  can be reformulated into a convex programming. In such cases, its gradient can be computed using existing implicit differential tools, see Amos & Kolter (2017) and Agrawal et al. (2019). In contrast, the term  $g(\theta)$  is non-smooth due to the indicator. To enable gradient-based optimization, we approximate the indicator with a smooth

surrogate  $\tilde{\mathbb{1}}\{a \leq b\} = \frac{1}{2}(1 + \text{erf}(\frac{b-a}{\sqrt{2}\sigma}))$ , where  $\text{erf}(x) = \frac{2}{\sqrt{\pi}} \int_0^x e^{-t^2} dt$  is the Gaussian error function and  $\sigma > 0$  controls the smoothness. Replacing the indicator in  $g(\theta)$  with this surrogate yields a smoothed constraint function  $\tilde{g}(\theta)$ . Similar smoothing techniques have been employed in the optimization problem of conformal prediction (Bai et al., 2022; Kiyani et al., 2024b). The resulting smoothed dual problem is given by:  $\min_{\theta \in \Theta} \max_{\lambda \geq 0} \tilde{L}(\lambda; \theta)$ , where  $\tilde{L}(\lambda; \theta) = f(\theta) + \lambda \tilde{g}(\theta)$ . This smooth approximation enables numerical solution via an alternating gradient descent algorithm. We refer to Davis et al. (2020) and Bolte et al. (2021) for the convergence analysis of similar optimization problems. Implementation details are summarized in Algorithm 1.

---

**Algorithm 1** Prediction Set Optimization with CRC

---

```

1: Input: Loss function  $\phi$ , robustness level  $1 - \alpha$ , labeled dataset  $\mathcal{D}_n = \{(X_i, Y_i)\}_{i=1}^n$ ,  

2: parametrized set  $\mathcal{U}_\theta(\cdot)$  with  $\theta \in \Theta$ , smooth surrogate function  $\tilde{\mathbb{1}}$ , learning rate  $\eta > 0$ .  

3: Initialize  $\theta \leftarrow \theta_0$  and  $\lambda = 0$ .  

4: Compute  $r_\theta(X_i)$  and  $z_\theta(X_i)$  for  $i \in [n]$ .  

5: Define empirical objective  $f(\theta)$  and set smooth constraint  $\tilde{g}(\theta)$ .  

6: Form the smoothed Lagrange multiplier  $\tilde{L}(\lambda; \theta) \leftarrow f(\theta) + \lambda \tilde{g}(\theta)$ .  

7: while no converged do  

8:   Perform a few steps of gradient descent on  $\theta$  to minimize  $\tilde{L}(\lambda; \theta)$ .  

9:   Compute  $\tilde{g}(\theta)$  and perform projected gradient ascent  $\lambda \leftarrow \max\{0, \lambda + \eta \tilde{g}(\theta)\}$ .  

10:  end while  

11:  $\hat{\theta} \leftarrow \theta$ .  

12: Output: Prediction set  $\mathcal{U}_{\hat{\theta}}(\cdot)$ .

```

---

**Remark 3.1.** In learning problems, Angelopoulos et al. (2024b) proposed the framework named *conformal risk control* by extending the miscoverage risk to general monotone risk functions. The robustness constraint can be regarded as a special risk, whereas it is not monotone in the model parameter. In addition, the objective function in Angelopoulos et al. (2024b) is the threshold parameter of prediction sets, but we consider the risk certificate function  $r(\cdot)$ , which is more complex.

### 3.3 THEORETICAL RESULTS

This section presents the theoretical guarantees for the solution to problem (6). The analysis for the smoothed variant (Algorithm 1), being conceptually analogous, are deferred to Appendix D.2. We equip the parameter space  $\Theta$  with the supremum norm and state the underlying assumptions.

**Condition 3.1.** *Loss function  $\phi$  is  $L_\phi$ -Lipschitz in decision  $z$  for any  $y \in \mathcal{Y}$ . For any  $x \in \mathcal{X}$ , the decision  $z_\theta(x)$  is  $L_z$ -Lipschitz in  $\theta$ . The risk certificate  $r_\theta(x)$  is  $L_r$ -Lipschitz in  $\theta \in \Theta$ , and uniformly bounded by a positive constant  $B_r > 0$  for any  $x \in \mathcal{X}$  and  $\theta \in \Theta$ .*

These regularity conditions are mild and typically satisfied in practice. For example, in portfolio optimization with the loss function  $\phi(y, z) = -y^\top z$ , the Lipschitz condition holds if  $\mathcal{Y}$  is bounded. For decision function  $z_\theta$  and risk certificate function  $r_\theta$ , if the CRO problem for prediction set  $\mathcal{U}_\theta$  can be transformed into a smooth convex optimization problem, then the Lipschitz property can be derived from the KKT conditions and the implicit function theorem, see Bolte et al. (2021) and Amos & Kolter (2017). The next assumption introduces a mild distributional assumption.

**Condition 3.2.** *Let  $V_\theta(X, Y) = \phi(Y, z_\theta(X)) - r_\theta(X)$  for data  $(X, Y) \sim P$ . Suppose that for all  $\theta \in \Theta$  the density of  $V_\theta(X, Y)$  is uniformly bounded by a constant  $\rho_0 > 0$ .*

The bounded density condition is often needed for concentration guarantees in the conformal prediction literature (Kiyani et al., 2024b; Jung et al., 2023; Lei & Wasserman, 2014).

**Definition 3.1 (Covering number).** *Let  $\Theta$  be a parameter space with the supremum norm  $\|\cdot\|_\infty$ . Given any  $\epsilon > 0$ , the subset  $\Theta_\epsilon \subseteq \Theta$  is called an  $\epsilon$ -covering of  $\Theta$  if for every  $\theta \in \Theta$ , there exists some  $\theta_\epsilon \in \Theta_\epsilon$  such that  $\|\theta - \theta_\epsilon\|_\infty < \epsilon$ . The covering number  $\mathcal{N}(\Theta, \|\cdot\|_\infty, \epsilon)$  is the smallest cardinality of any  $\epsilon$ -covering of  $\Theta$ .*

Covering numbers quantify the complexity of a function class and are a fundamental tool in statistical learning theory and convergence analysis (Van Der Vaart & Wellner, 1996). The next two

270 theorems provide a non-asymptotic characterization of the robustness and expected risk certificate  
 271 value for CRC.

272 **Theorem 3.2 (Robustness gap).** *Let  $\hat{\theta}$  be the solution to optimization problem (6). Under Conditions 273 3.1 and 3.2, for any independent data  $(X, Y) \sim P$ , conditioning on the labeled data  $\mathcal{D}_n$ , the 274 following inequality holds: with probability at least  $1 - n^{-1}$ ,*

$$276 \mathbb{P} \{ \phi(Y, z_{\hat{\theta}}(X)) \leq r_{\hat{\theta}}(X) \mid \mathcal{D}_n \} \geq 1 - \alpha - \Delta_n, \\ 277$$

278 where the robustness gap  $\Delta_n = 5\sqrt{\frac{\log(2\mathcal{N}(\Theta, \|\cdot\|_{\infty}, n^{-1})) + \log n}{2n}} + \frac{4(L_{\phi}L_z + L_r)\rho_0}{n}$ .  
 279

280 **Theorem 3.3 (Risk certificate optimality).** *Let  $\theta_{\Delta_n}^*$  denote the optimal solution of problem (5) at 281 the robustness level  $1 - \alpha + \Delta_n$ . Under the same conditions as Theorem 3.2, conditioning on  $\mathcal{D}_n$ , 282 with probability at least  $1 - 2n^{-1}$ ,*

$$283 \mathbb{E} \left[ r_{\hat{\theta}}(X) - r_{\theta_{\Delta_n}^*}(X) \mid \mathcal{D}_n \right] \leq 4B_r \sqrt{\frac{\log(2\mathcal{N}(\Theta, \|\cdot\|_{\infty}, n^{-1})) + \log n}{2n}} + \frac{4L_r}{n}. \\ 284 \\ 285$$

286 For a finite-dimensional parameter space  $\Theta$  of dimension  $d$ , the covering number scales approximately 287 as  $\mathcal{N}(\Theta, \|\cdot\|_{\infty}, n^{-1}) \asymp n^d$ , so both the robustness gap and the expected risk certificate 288 converge to zero at rate  $O(\sqrt{d \log n / n})$ . In Appendix D, we provide more comprehensive theoretical 289 results, such as in the setting where the function class has a finite VC dimension.  
 290

291 **Remark 3.2.** *It is worth noting that  $\theta_{\Delta_n}^*$  denotes the optimal model under a slightly relaxed robustness 292 level  $1 - \alpha + \Delta_n$ , rather than the exact level  $1 - \alpha$ . This relaxation is introduced to ensure that 293  $\theta_{\Delta_n}^*$  is feasible to the problem (6) with high probability, thereby guaranteeing that the empirical risk 294 certificate of  $\hat{\theta}$  is less than that of  $\theta_{\Delta_n}^*$  with high probability. Finally, leveraging relevant theories of 295 empirical process, we can establish the bounds in Theorems 3.2 and 3.3. Let  $\theta^*$  be the solution to the 296 problem (4). If additional assumptions are imposed regarding the  $\|\theta_{\Delta_n}^* - \theta^*\|_{\infty}$ , such a relaxation 297 may no longer be needed.*

## 299 4 TEST-TIME DECISION WITH FINITE-SAMPLE ROBUSTNESS CONTROL

301 In this section, we turn to the practical task of making decisions at a *test point*  $X_{n+1}$  with unknown  
 302 label  $Y_{n+1}$ . A straightforward approach is to output the decision  $z_{\mathcal{U}_{\hat{\theta}}}(X_{n+1})$ , where  $\hat{\theta}$  is solution  
 303 to the problem (6). Theorem 3.2 shows that the robustness of the decision  $z_{\mathcal{U}_{\hat{\theta}}}(X_{n+1})$  converges to  
 304 the target level asymptotically. To achieve *finite-sample* robustness control for the decision of the  
 305 specific test point, we further calibrate the prediction set obtained from Algorithm 1 using both the  
 306 test data  $X_{n+1}$  and the labeled data  $\{(X_i, Y_i)\}_{i=1}^n$ .

307 Specifically, we split the labeled dataset  $\mathcal{D}_n$  into a training set  $\mathcal{D}_{\text{train}} = \{(X_i, Y_i)\}_{i=1}^{n_0}$  and a calibration  
 308 set  $\mathcal{D}_{\text{cal}} = \{(X_i, Y_i)\}_{i=n_0+1}^n$ , where  $n_0 < n$ . We first obtain the optimized prediction set  $\mathcal{U}_{\hat{\theta}_0}(\cdot)$   
 309 using only  $\mathcal{D}_{\text{train}}$  in Algorithm 1. Next, we apply full conformal prediction (Vovk et al., 2005; Lei  
 310 et al., 2018) to calibrate the prediction set  $\mathcal{U}_{\hat{\theta}_0}(\cdot)$  based on  $\mathcal{D}_{\text{cal}}$  and  $X_{n+1}$ .  
 311

312 Calibrating the entire parameters  $\theta$  is computationally expensive and often unnecessary. Instead,  
 313 we can adjust the prediction set  $\mathcal{U}_{\hat{\theta}_0}(\cdot)$  by tuning a single radius parameter  $t \in \mathbb{R}^+$ , which controls  
 314 the size of the set and provides an efficient way of model calibration. Following the framework of  
 315 nested prediction set in Gupta et al. (2022), we call the family  $\{\mathcal{U}_{\theta,t}(x)\}_{t \in \mathbb{R}^+}$  *nested sets* if  $t_1 \leq t_2$   
 316 implies that  $\mathcal{U}_{\theta,t_1}(x) \subseteq \mathcal{U}_{\theta,t_2}(x)$  for any  $x \in \mathcal{X}$ . For the two examples of prediction sets in Section  
 317 3.1, the nested versions are given as follows.  
 318

- Nested parametrized box set:

$$320 \mathcal{U}_{\theta,t}(x) = \{y \in \mathbb{R}^q : h_{\theta}^{\text{lo}}(x) - t \leq y \leq h_{\theta}^{\text{hi}}(x) + t\}; \\ 321$$

- Nested parametrized ellipsoidal set:

$$322 \mathcal{U}_{\theta,t}(x) = \{y \in \mathbb{R}^q : (y - \mu_{\theta}(x))^{\top} \Sigma_{\theta}^{-1}(x) (y - \mu_{\theta}(x)) \leq t\}. \\ 323$$

Let  $y \in \mathcal{Y}$  be a *hypothesized value* for the test label  $Y_{n+1}$ , and denote the augmented calibration set as  $\{(X_i, Y_i^y)\}_{i=n_0+1}^{n+1}$ , where  $Y_i^y = Y_i$  for  $n_0 + 1 \leq i \leq n$  and  $Y_{n+1}^y = y$ . Given the prediction set  $\mathcal{U}_{\hat{\theta}_0, t}(\cdot)$ , the hypothesized radius threshold is computed by

$$\hat{t}^y = \min \left\{ t \in \mathbb{R}^+ : \frac{1}{n - n_0 + 1} \sum_{i=n_0+1}^{n+1} \mathbb{1} \left\{ \phi(Y_i^y, z_{\hat{\theta}_0, t}(X_i)) \leq r_{\hat{\theta}_0, t}(X_i) \right\} \geq 1 - \alpha \right\}, \quad (7)$$

where  $z_{\theta, t}(x) := \arg \min_{z \in \mathcal{Z}} \max_{c \in \mathcal{U}_{\theta, t}(x)} \phi(c, z)$  and  $r_{\theta, t}(x) := \max_{c \in \mathcal{U}_{\theta, t}(x)} \phi(c, z_{\theta, t}(x))$ . Then the calibrated prediction set is given by

$$\mathcal{U}_{\text{Cal}}(X_{n+1}) = \left\{ y \in \mathcal{Y} : \phi(y, z_{\hat{\theta}_0, \hat{t}^y}(X_{n+1})) \leq r_{\hat{\theta}_0, \hat{t}^y}(X_{n+1}) \right\}.$$

Finally, the decision for test point is made by  $z_{\mathcal{U}_{\text{Cal}}}(X_{n+1})$ . We name the procedure above as Calibrated CRC (Cal-CRC), and summarize it in Algorithm 2.

---

**Algorithm 2** Cal-CRC

---

```

1: Input: Same as Algorithm 1, size of training set  $n_0$ , and test point  $X_{n+1}$ .
2: Sample splitting:  $\mathcal{D}_{\text{train}} = \{(X_i, Y_i)\}_{i=1}^{n_0}$  and  $\mathcal{D}_{\text{cal}} = \{(X_i, Y_i)\}_{i=n_0+1}^n$ .
3: Training: Obtain the prediction set  $\mathcal{U}_{\hat{\theta}_0}(\cdot)$  by running Algorithm 1 on  $\mathcal{D}_{\text{train}}$ .
4: Calibration:  $\mathcal{U}_{\text{Cal}}(X_{n+1}) \leftarrow \emptyset$ .
5: for  $y \in \mathcal{Y}$  do
6:   Define  $\{(X_i, Y_i^y)\}_{i=n_0+1}^{n+1}$ , where  $Y_i^y = Y_i$  for  $n_0 + 1 \leq i \leq n$  and  $Y_{n+1}^y = y$ .
7:   Calculate the hypothesized threshold  $\hat{t}^y$  via (7).
8:   if  $\phi(y, z_{\hat{\theta}_0, \hat{t}^y}(X_{n+1})) \leq r_{\hat{\theta}_0, \hat{t}^y}(X_{n+1})$  then
9:      $\mathcal{U}_{\text{Cal}}(X_{n+1}) \leftarrow \mathcal{U}_{\text{Cal}}(X_{n+1}) \cup \{y\}$ .
10:  end if
11: end for
12: Make the decision:  $z_{\mathcal{U}_{\text{Cal}}}(X_{n+1}) \leftarrow \arg \min_{z \in \mathcal{Z}} \max_{y \in \mathcal{U}_{\text{Cal}}(X_{n+1})} \phi(y, z)$ .
13: Output: the decision  $z_{\mathcal{U}_{\text{Cal}}}(X_{n+1})$ .

```

---

**Theorem 4.1.** *If the labeled data  $\{(X_i, Y_i)\}_{i=1}^n$  and test data  $(X_{n+1}, Y_{n+1})$  are i.i.d., then we have the finite-sample robustness guarantee*

$$\mathbb{P} \{ \phi(Y_{n+1}, z_{\mathcal{U}_{\text{Cal}}}(X_{n+1})) \leq r_{\mathcal{U}_{\text{Cal}}}(X_{n+1}) \} \geq 1 - \alpha.$$

The finite-sample robustness relies solely on the exchangeability of data, which is identical to that in classical conformal prediction theory (Lei et al., 2018). For implementation, note that the calibrated prediction set  $\mathcal{U}_{\text{Cal}}(X_{n+1})$  is obtained by traversing all possible values of  $y \in \mathcal{Y}$ . In practice, we can apply the discretization technique (Chen et al., 2018) to avoid exhaustive search. The complete implementation is provided in the Appendix B.4. The decision optimality of  $z_{\mathcal{U}_{\text{Cal}}}$  is analyzed in the Appendix B.5, and corresponding simulation results will be provided in Section E.3.

## 5 EXPERIMENTS

In this section, we compare our proposed CRC with two baseline methods for robust decision-making: (i) CRO with conformal prediction sets (Sun et al., 2023); (ii) End-to-end (E2E) method (Chenreddy & Delage, 2024; Yeh et al., 2024) to minimize the expected risk certificate. For clarity, we refer to the application of CRC to ellipsoidal prediction sets as CRC-E, and to box prediction sets as CRC-B. The same naming convention is applied to the CRO and E2E methods for consistency. The implementation details of each baseline method are given in Appendix E.2.

We utilize the following metrics to evaluate the performance of three methods. (i) **Risk Certificate**: The average of  $r_{\mathcal{U}}(X)$  across all test samples; (ii) **Decision Loss**: The average of  $\phi(Y, z_{\mathcal{U}}(X))$  across all test samples; (iii) **Robustness**: The proportion of test samples where  $\phi(Y, z_{\mathcal{U}}(X))$  is less or equal to  $r_{\mathcal{U}}(X)$ ; (iv) **Coverage**: The proportion of test samples where the true label  $Y$  is covered by the prediction set  $\mathcal{U}(X)$ .

378  
379

## 5.1 SYNTHETIC DATA ON PORTFOLIO OPTIMIZATION

380  
381  
382

In this simulation, we define the loss function as  $\phi(y, z) = -y^\top z$ , where  $\mathcal{Y} = \mathbb{R}^2$  and  $\mathcal{Z} = \{z \in [0, 1]^2 : \|z\|_1 = 1\}$ . The labeled data and test data are generated by:

383  
384

$$Y_1 = -5X_1 - 2X_2^2 - e_1, \quad Y_2 = -3X_1^2 - X_2 - e_2,$$

385  
386  
387  
388  
389

where  $Y = (Y_1, Y_2)$ ,  $X = (X_1, X_2)$ , and  $e = (e_1, e_2)$ . The covariate  $X \sim N((1, 1)^\top, 2.25 \cdot I_2)$ , where  $I_2$  is a 2-dimensional identity matrix. The noise  $e \sim N(0, I_2)$  is independent of  $X$ . We only consider ellipsoidal prediction sets since the oracle prediction set of  $Y \mid X$  is ellipsoidal under the normal noise setting. Further experimental details will be presented in Appendix E.1. All methods are evaluated over 100 trials, and the average results are reported.

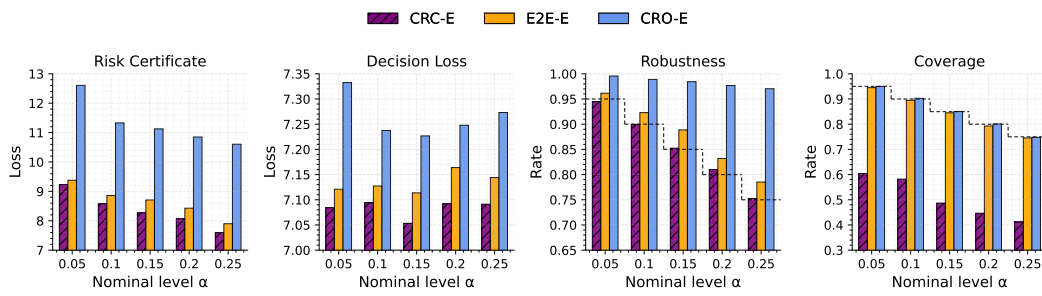
390  
391  
392  
393  
394  
395  
396  
397  
398  
399  
400401  
402  
403  
404

Figure 2: The results of risk certificate, decision loss, robustness, and coverage on synthetic data when varying nominal level  $\alpha$  with identical sample size  $n = 1500$ . The horizontal gray dashed lines refer to robustness levels. The prediction sets are ellipsoids.

405  
406  
407  
408  
409  
410  
411  
412  
413

**Results.** We evaluate the decision performance of CRC and the baseline methods by varying the nominal level  $\alpha$ . As shown in Figure 2, CRC consistently outperforms the baselines in both risk certificate and decision loss. In addition, CRC also maintains the robustness level to the nominal target, while the baseline methods tend to be more conservative. With respect to coverage, CRC attains a much lower coverage rate than the robustness level, which verifies the motivation of our method. Additionally, the results for varying sample sizes are shown in Figure 3. CRC-E continues to show strong performance across all metrics, demonstrating its stable advantage. In Figure 6 of Appendix E.3, we present the density plots for risk certificate and decision loss when  $\alpha = 0.15$ . The overall density of CRC is shifted towards the lower loss region, further validating its superiority.

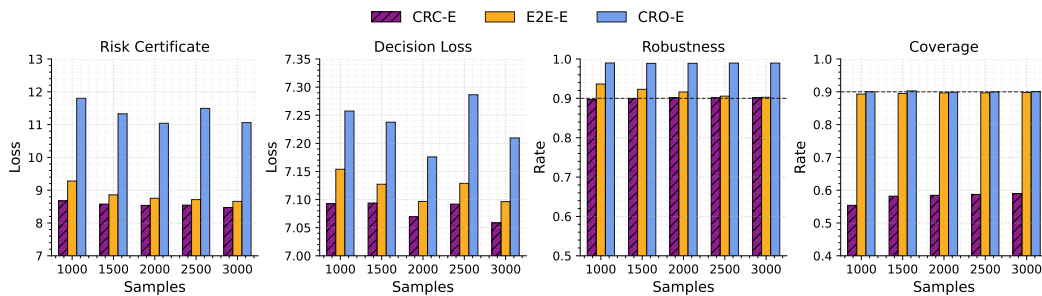
414  
415  
416  
417  
418  
419  
420  
421  
422  
423  
424425  
426  
427

Figure 3: The results of risk certificate, decision loss, robustness, and coverage on synthetic data when varying sample size  $n$  with identical nominal level  $\alpha = 0.1$ .

428  
429  
430  
431

Since the RAC method proposed Kiyani et al. (2025) is applicable to discrete decision space in classification problem, we conduct the simulation on RAC method by discretizing the label space  $\mathcal{Y}$  and decision space  $\mathcal{Z}$ . The results are provided in Appendix E.4. In addition, we also report the simulation results under the polyhedral prediction set in Appendix E.6.

432 5.2 US STOCK PROBLEM  
433

434 We conduct an additional experiment on the portfolio optimization problem using a real-world  
435 dataset, following the experimental design outlined in Chenreddy et al. (2022). The dataset com-  
436 prises historical US stock market data from January 1, 2012, to December 31, 2020, covering 64  
437 stocks across eight different sectors. Daily percentage gains or losses are computed from the ad-  
438 justed closing prices of consecutive trading days and used as labels. To enhance the input infor-  
439 mation for the model, we also incorporate the trading volume of individual stocks and several market  
440 benchmark indices as covariates. To evaluate the robustness of the methodology, we randomly se-  
441 lect 15 stocks from the pool of 64 as the investable asset set in each experiment and repeat the  
442 process multiple times to mitigate the influence of random chance. We define the loss function as  
443  $\phi(y, z) = -y^\top z$ , where  $\mathcal{Y} = \mathbb{R}^q$  and  $\mathcal{Z} = \{z \in [0, 1]^q : \|z\|_1 = 1, z \geq 0\}$ .  
444

445 Table 1: The results of risk certificate, decision loss, and robustness under nominal levels  $\alpha = 0.1$   
446 and  $\alpha = 0.2$  on the US stock problem.

Method	Nominal level $\alpha = 0.1$			Nominal level $\alpha = 0.2$		
	Risk Certificate	Decision Loss	Robustness (%)	Risk Certificate	Decision Loss	Robustness (%)
CRC-B	<b>1.160</b>	<b>-0.055</b>	<b>90.9</b>	<b>0.731</b>	<b>-0.059</b>	<b>80.6</b>
CRO-B	3.794	-0.051	99.9	3.017	-0.054	99.5
E2E-B	2.129	-0.046	96.7	1.512	-0.041	92.7
CRC-E	<b>1.028</b>	<b>-0.077</b>	<b>90.8</b>	<b>0.701</b>	<b>-0.075</b>	<b>80.6</b>
CRO-E	6.345	-0.069	99.9	6.195	-0.046	99.8
E2E-E	4.995	-0.071	98.6	4.503	-0.070	96.4

455 **Results.** As shown in Table 1, CRC outperforms the baseline methods in both risk certification and  
456 decision loss. In terms of robustness, CRC maintains a level close to the target  $1 - \alpha$ , demonstrating  
457 strong stability and adaptability. In contrast, E2E and CRO frequently exceed the nominal robustness  
458 target, which indicates the adoption of overly conservative strategies that lead to higher losses and  
459 risks. Overall, CRC achieves a superior balance between risk control and decision performance.  
460

461 5.3 BATTERY STORAGE PROBLEM  
462

463 In this subsection, we consider a battery storage control problem based on the frameworks of Donti  
464 et al. (2017) and Yeh et al. (2024). Given hourly electricity price forecasts  $y \in \mathbb{R}^T$  and contextual  
465 covariates over a  $T$ -hour horizon, the controller determines the charging power  $z^{\text{in}} \in \mathbb{R}^T$ , discharg-  
466 ing power  $z^{\text{out}} \in \mathbb{R}^T$ , and the resulting state of charge  $z^{\text{state}} \in \mathbb{R}^T$ , subject to the constraints for  
467  $t = 1, \dots, T$ :

$$z_0^{\text{state}} = \frac{B}{2}, \quad z_t^{\text{state}} = z_{t-1}^{\text{state}} - z_t^{\text{out}} + \gamma z_t^{\text{in}}, \\ 0 \leq z_t^{\text{in}} \leq c^{\text{in}}, \quad 0 \leq z_t^{\text{out}} \leq c^{\text{out}}, \quad 0 \leq z_t^{\text{state}} \leq B.$$

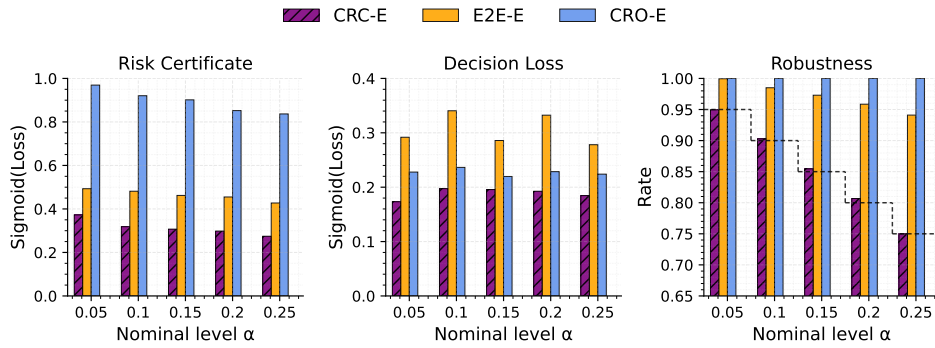
471 Here  $B$  denotes battery capacity,  $\gamma$  denotes charging efficiency, and  $c^{\text{in}}, c^{\text{out}}$  denotes per-hour power  
472 limits. The objective balances three key factors: (1) Profit from arbitrage, which involves buying  
473 and selling energy based on the prices  $y \in \mathbb{R}^T$ ; (2) Flexibility, which is encouraged by maintaining  
474 the battery's state of charge close to half of its total capacity; (3) Battery health, which is preserved  
475 by penalizing large charging and discharging magnitudes. The resulting loss function is:  
476

$$\phi(y, z) = \sum_{t=1}^T y_t (z_t^{\text{in}} - z_t^{\text{out}}) + \beta \left\| z^{\text{state}} - \frac{B}{2} \mathbf{1} \right\|_2^2 + \varepsilon (\|z^{\text{in}}\|_2^2 + \|z^{\text{out}}\|_2^2),$$

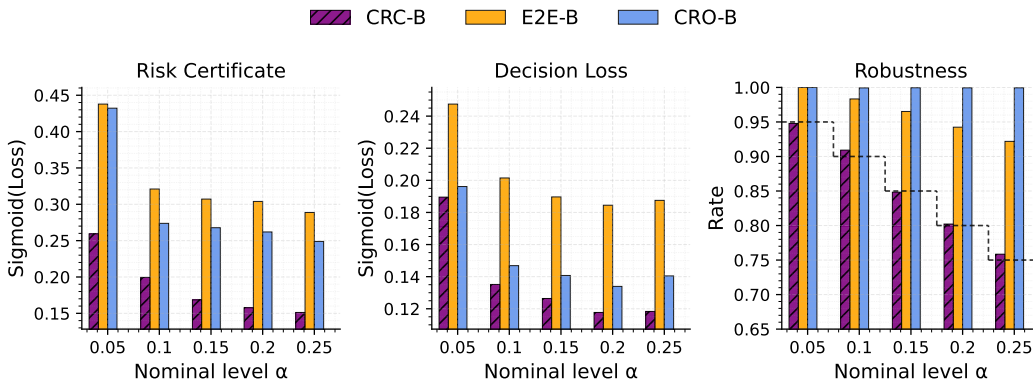
480 Following Donti et al. (2017) and Yeh et al. 2024, we also set  $T = 24$  hours,  $B = 1$ ,  $\gamma = 0.9$ ,  
481  $c^{\text{in}} = 0.5$ ,  $c^{\text{out}} = 0.2$ ,  $\beta = 0.1$ , and  $\varepsilon = 0.05$ .

482 **Results.** Figure 4 presents a comparative analysis of the CRC method against the baselines using  
483 ellipsoidal prediction sets. For clearer visualization, negative indicator values are mapped onto the  
484 positive half-axis via a sigmoid transformation. The results demonstrate CRC's consistent superi-  
485 ority over both E2E and CRO across all three key metrics. As the nominal level increases, CRC  
effectively mitigates risk in all measures, sustaining the lowest risk and loss values at higher levels.  
486

486 In addition, CRC maintains robustness values close to the nominal target, highlighting its stability  
 487 and adaptability. In contrast, E2E and CRO consistently exceed the robustness target, leading to  
 488 decisions characterized by excessive conservatism. The results of the box prediction set is presented  
 489 in Figure 5.



503 Figure 4: The results of risk certificate, decision loss, and robustness when varying nominal level  $\alpha$   
 504 on battery storage problem. The prediction sets are ellipsoids.



520 Figure 5: The risk certificate, decision loss and robustness when varying nominal level  $\alpha$  on battery  
 521 storage problem. The prediction sets are box.

## 524 6 CONCLUSION AND DISCUSSION

526 This paper introduces Conformal Robustness Control (CRC), a novel framework that optimizes the  
 527 construction of prediction sets for robust decision-making by directly minimizing the expected risk  
 528 certificate under robustness constraints. Unlike existing conditional robust optimization methods  
 529 with conformal prediction sets, CRC adopts robustness constraints instead of coverage constraints,  
 530 expanding the range of feasible prediction sets and enabling more efficient decisions. Theoretical  
 531 guarantees for both robustness and optimality are provided, and empirical results on real-world  
 532 data demonstrate significant improvements over baseline methods. Our work also identifies future  
 533 research directions in data-driven robust optimization, such as developing more efficient strategies  
 534 to solve the optimization problem and designing domain-specific parameterizations of prediction  
 535 sets to achieve higher-quality decisions in practical applications.

540 REFERENCES  
541

542 Akshay Agrawal, Brandon Amos, Shane Barratt, Stephen Boyd, Steven Diamond, and J Zico Kolter.  
543 Differentiable convex optimization layers. *Advances in Neural Information Processing Systems*,  
544 32, 2019.

545 Brandon Amos and J Zico Kolter. Optnet: Differentiable optimization as a layer in neural networks.  
546 In *International Conference on Machine Learning*, pp. 136–145. PMLR, 2017.

547 Anastasios N Angelopoulos, Rina Foygel Barber, and Stephen Bates. Theoretical foundations of  
548 conformal prediction. *arXiv preprint arXiv:2411.11824*, 2024a.

549 Anastasios N Angelopoulos, Stephen Bates, Adam Fisch, Lihua Lei, and Tal Schuster. Conformal  
550 risk control. In *The Twelfth International Conference on Learning Representations*, 2024b.

551 Yu Bai, Song Mei, Huan Wang, Yingbo Zhou, and Caiming Xiong. Efficient and differentiable  
552 conformal prediction with general function classes. In *International Conference on Learning  
553 Representations*, 2022.

554 Yajie Bao, Yang Hu, Haojie Ren, Peng Zhao, and Changliang Zou. Optimal model selection for  
555 conformalized robust optimization. *arXiv preprint arXiv:2507.04716*, 2025.

556 Andreas Bärmann, Andreas Heidt, Alexander Martin, Sebastian Pokutta, and Christoph Thurner.  
557 Polyhedral approximation of ellipsoidal uncertainty sets via extended formulations: a computa-  
558 tional case study. *Computational Management Science*, 13(2):151–193, 2016.

559 A. Ben-Tal, L.E. Ghaoui, and A. Nemirovski. *Robust Optimization*. Princeton Series in Applied  
560 Mathematics. Princeton University Press, 2009. ISBN 9781400831050.

561 Dimitris Bertsimas, Vishal Gupta, and Nathan Kallus. Data-driven robust optimization. *Mathemat-  
562 ical Programming*, 167(2):235–292, 2018.

563 Jérôme Bolte, Tam Le, Edouard Pauwels, and Tony Silveti-Falls. Nonsmooth implicit differentation  
564 for machine-learning and optimization. *Advances in Neural Information Processing Systems*, 34:  
565 13537–13549, 2021.

566 Wenyu Chen, Kelli-Jean Chun, and Rina Foygel Barber. Discretized conformal prediction for effi-  
567 cient distribution-free inference. *Stat*, 7(1):e173, 2018.

568 Abhilash Reddy Chenreddy and Erick Delage. End-to-end conditional robust optimization. In  
569 *Proceedings of the Fortieth Conference on Uncertainty in Artificial Intelligence*, volume 244, pp.  
570 736–748. PMLR, 15–19 Jul 2024.

571 Abhilash Reddy Chenreddy, Nymisha Bandi, and Erick Delage. Data-driven conditional robust  
572 optimization. *Advances in Neural Information Processing Systems*, 35:9525–9537, 2022.

573 Damek Davis, Dmitriy Drusvyatskiy, Sham Kakade, and Jason D Lee. Stochastic subgradient  
574 method converges on tame functions. *Foundations of Computational Mathematics*, 20(1):119–  
575 154, 2020.

576 Priya Donti, Brandon Amos, and J Zico Kolter. Task-based end-to-end model learning in stochastic  
577 optimization. *Advances in Neural Information Processing Systems*, 30:5490 – 5500, 2017.

578 Laurent El Ghaoui, Maksim Oks, and Francois Oustry. Worst-case value-at-risk and robust portfolio  
579 optimization: A conic programming approach. *Operations Research*, 51(4):543–556, 2003.

580 Chirag Gupta, Arun K Kuchibhotla, and Aaditya Ramdas. Nested conformal prediction and quantile  
581 out-of-bag ensemble methods. *Pattern Recognition*, 127:108496, 2022.

582 L Jeff Hong, Zhiyuan Huang, and Henry Lam. Learning-based robust optimization: Procedures and  
583 statistical guarantees. *Management Science*, 67(6):3447–3467, 2021.

584 Ulf Johansson, Henrik Linusson, Tuve Löfström, and Henrik Boström. Model-agnostic nonconfor-  
585 mity functions for conformal classification. In *2017 International Joint Conference on Neural  
586 Networks (IJCNN)*, pp. 2072–2079. IEEE, 2017.

594 Chancellor Johnstone and Bruce Cox. Conformal uncertainty sets for robust optimization. In *Con-*  
 595 *formal and Probabilistic Prediction and Applications*, pp. 72–90. PMLR, 2021.  
 596

597 Christopher Jung, Georgy Noarov, Ramya Ramalingam, and Aaron Roth. Batch multivalid confor-  
 598 *mal prediction*. In *International Conference on Learning Representations*, 2023.

599 Shayan Kiyani, George Pappas, and Hamed Hassani. Conformal prediction with learned features.  
 600 *arXiv preprint arXiv:2404.17487*, 2024a.  
 601

602 Shayan Kiyani, George J Pappas, and Hamed Hassani. Length optimization in conformal prediction.  
 603 *Advances in Neural Information Processing Systems*, 37:99519–99563, 2024b.  
 604

605 Shayan Kiyani, George Pappas, Aaron Roth, and Hamed Hassani. Decision theoretic foundations for  
 606 *conformal prediction: Optimal uncertainty quantification for risk-averse agents*. *arXiv preprint*  
 607 *arXiv:2502.02561*, 2025.

608 Jing Lei and Larry Wasserman. Distribution-free prediction bands for non-parametric regression.  
 609 *Journal of the Royal Statistical Society Series B: Statistical Methodology*, 76(1):71–96, 2014.  
 610

611 Jing Lei, Max G’Sell, Alessandro Rinaldo, Ryan J Tibshirani, and Larry Wasserman. Distribution-  
 612 *free predictive inference for regression*. *Journal of the American Statistical Association*, 113  
 613 (523):1094–1111, 2018.

614 Ruiting Liang, Wanrong Zhu, and Rina Foygel Barber. Conformal prediction after efficiency-  
 615 *oriented model selection*. *arXiv preprint arXiv:2408.07066*, 2024.

616 Harry Markowitz. Portfolio selection. *The Journal of Finance*, 7(1):77–91, 1952.  
 617

618 Pascal Massart. The tight constant in the dvoretzky-kiefer-wolfowitz inequality. *The Annals of*  
 619 *Probability*, pp. 1269–1283, 1990.  
 620

621 Karthik Natarajan, Dessislava Pachamanova, and Melvyn Sim. Incorporating asymmetric distri-  
 622 *butional information in robust value-at-risk optimization*. *Management Science*, 54(3):573–585,  
 623 2008.

624 Harris Papadopoulos, Kostas Proedrou, Volodya Vovk, and Alex Gammerman. Inductive confidence  
 625 *machines for regression*. In *Machine Learning: ECML 2002: 13th European Conference on*  
 626 *Machine Learning Helsinki, Finland*, pp. 345–356. Springer, 2002.  
 627

628 Yash P Patel, Sahana Rayan, and Ambuj Tewari. Conformal contextual robust optimization. In  
 629 *International Conference on Artificial Intelligence and Statistics*, pp. 2485–2493. PMLR, 2024.

630 R Tyrrell Rockafellar and Stanislav Uryasev. Conditional value-at-risk for general loss distributions.  
 631 *Journal of Banking & Finance*, 26(7):1443–1471, 2002.  
 632

633 Mauricio Sadinle, Jing Lei, and Larry Wasserman. Least ambiguous set-valued classifiers with  
 634 *bounded error levels*. *Journal of the American Statistical Association*, 114(525):223–234, 2019.  
 635

636 Chao Shang, Xiaolin Huang, and Fengqi You. Data-driven robust optimization based on kernel  
 637 *learning*. *Computers & Chemical Engineering*, 106:464–479, 2017.  
 638

639 David Stutz, Krishnamurthy Dj Dvijotham, Ali Taylan Cemgil, and Arnaud Doucet. Learning opti-  
 640 *mal conformal classifiers*. In *International Conference on Learning Representations*, 2022.  
 641

642 Chunlin Sun, Linyu Liu, and Xiaocheng Li. Predict-then-calibrate: a new perspective of robust  
 643 *contextual LP*. *Advances in Neural Information Processing Systems*, 36:17713–17741, 2023.  
 644

645 Stanislav Uryasev and R Tyrrell Rockafellar. Conditional value-at-risk: optimization approach. In  
 646 *Stochastic Optimization: Algorithms and Applications*, pp. 411–435. Springer, 2001.  
 647

648 Aad W Van Der Vaart and Jon A Wellner. Weak convergence. In *Weak convergence and empirical*  
 649 *processes: with applications to statistics*, pp. 16–28. Springer, 1996.  
 650

651 Vladimir Vovk, Alexander Gammerman, and Glenn Shafer. *Algorithmic learning in a random world*.  
 652 Springer, 2005.

648 Irina Wang, Cole Becker, Bart Van Parys, and Bartolomeo Stellato. Learning decision-focused  
649 uncertainty sets in robust optimization. *arXiv preprint arXiv:2305.19225*, 2023.  
650

651 Yachong Yang and Arun Kumar Kuchibhotla. Selection and aggregation of conformal prediction  
652 sets. *Journal of the American Statistical Association*, 120(549):435–447, 2025.

653 Christopher Yeh, Nicolas Christianson, Alan Wu, Adam Wierman, and Yisong Yue. End-to-end  
654 conformal calibration for optimization under uncertainty. *arXiv preprint arXiv:2409.20534*, 2024.

655

656

657

658

659

660

661

662

663

664

665

666

667

668

669

670

671

672

673

674

675

676

677

678

679

680

681

682

683

684

685

686

687

688

689

690

691

692

693

694

695

696

697

698

699

700

701

702 **A USAGE STATEMENT OF LARGE LANGUAGE MODEL**  
 703

704 We used a large language model solely for improving the fluency and readability of the manuscript.  
 705 The model was not involved in research ideation, experimental design, data analysis, or result inter-  
 706 pretation. All scientific contributions and substantive content were solely produced by the authors.  
 707

708 **B MORE DISCUSSION ON RELATED WORK**  
 709

710 **B.1 RELATIONSHIP BETWEEN THE CRC PROBLEM AND THE VaR PROBLEM**  
 711

712 The following proposition illustrates the relationship between the VaR problem and the CRC prob-  
 713 lem (4).  
 714

**Proposition B.1.** *Let  $z^Q(X) = \arg \min_{z \in \mathcal{Z}} \text{VaR}_{1-\alpha}(\phi(Y, z) \mid X)$  be the unique minimizer of VaR  
 715 problem. There exists a prediction set  $\mathcal{U}^Q$  such that  $z_{\mathcal{U}^Q} = z^Q$ . Moreover, the robustness constraint  
 716 is satisfied:*

$$717 \mathbb{P}[\phi(Y, z_{\mathcal{U}^Q}(X)) \leq r_{\mathcal{U}^Q}(X)] \geq 1 - \alpha.$$

718 Furthermore, there exist cases where  $z^Q = z_{\mathcal{U}^*}$ , with  $\mathcal{U}^*$  being the solution to optimization problem  
 719 (4), and cases where  $z^Q \neq z_{\mathcal{U}^*}$ .  
 720

721 The above conclusion indicates that, at least in some cases, decision  $z_{\mathcal{U}^*}$  and decision  $z^Q$  are con-  
 722 sistent. When decision  $z_{\mathcal{U}^*}$  and decision  $z^Q$  are inconsistent, the expected risk certificate generated by  
 723 decision  $z_{\mathcal{U}^*}$  will also be lower than that of  $z^Q$ , indicating that  $z_{\mathcal{U}^*}$  still holds practical significance.  
 724

725 *Proof of Proposition B.1.* To find a prediction set  $\mathcal{U}^Q$  such that  $z^Q$  equals  $z_{\mathcal{U}^Q}$ , it is sufficient to  
 726 define prediction set  $\mathcal{U}^Q$  in the following form:  
 727

$$728 \mathcal{U}^Q(x) = \{y \in \mathcal{Y} : \phi(y, z^Q(x)) \leq \text{VaR}_{1-\alpha}(\phi(Y, z^Q(X)) \mid X = x)\}, \quad \forall x \in \mathcal{X}.$$

729 Next, we will proceed with the verification. Since the coverage constraint is a sufficient condition  
 730 for the robustness constraint, we have  
 731

$$732 \mathbb{P}\{\phi(Y, z_{\mathcal{U}^Q}(X)) \leq r_{\mathcal{U}^Q}(X)\} \geq \mathbb{P}\{Y \in \mathcal{U}^Q(X)\} \\ 733 = \mathbb{P}\{\phi(Y, z^Q(X)) \leq \text{VaR}_{1-\alpha}(\phi(Y, z^Q(X)) \mid X)\} \\ 734 \geq 1 - \alpha.$$

736 Thus, we verify that robustness holds. Secondly, based on the definition of quantiles, we  
 737 have  $\mathbb{P}\{Y \in \mathcal{U}^Q(x)\} \geq 1 - \alpha, \forall x \in \mathcal{X}$ . Therefore, we can control the upper bound of  
 738  $\text{VaR}_{1-\alpha}(\phi(Y, z_{\mathcal{U}^Q}(X)) \mid X = x)$  in the following way:  
 739

$$740 \text{VaR}_{1-\alpha}(\phi(Y, z_{\mathcal{U}^Q}(X)) \mid X = x) \leq \max_{y \in \mathcal{U}^Q(x)} \phi(y, z_{\mathcal{U}^Q}(x)) \\ 741 \leq \max_{y \in \mathcal{U}^Q(x)} \phi(y, z^Q(x)) \\ 742 \leq \text{VaR}_{1-\alpha}(\phi(Y, z^Q(X)) \mid X = x).$$

745 That is,  $z_{\mathcal{U}^Q}$  is also the optimal solution in the sense of minimizing the  $1 - \alpha$  quantile. Therefore,  
 746  $z_{\mathcal{U}^Q}$  equals  $z^Q$  if  $z^Q$  is the unique optimal solution.  
 747

For the scenario where decision  $z^Q$  is equal to decision  $z_{\mathcal{U}^*}$ , consider the following example. Let  
 748  $\mathcal{X} = \{0, 1\}$  and  $\mathcal{Z} = \{0, 1\}$ . Suppose that the density of  $\phi(Y, z)$  given  $X = x$  is as follows.  
 749

750 For  $x \in \{0, 1\}$ ,  $z = 0$ , the density is  
 751

$$752 f(\phi) = \frac{1}{25} [3\mathbb{I}\{0 \leq \phi < 7.5\} + \mathbb{I}\{7.5 \leq \phi < 10\}].$$

753 For  $x \in \{0, 1\}$ ,  $z = 1$ , the density is  
 754

$$755 f(\phi) = \frac{1}{25} [\mathbb{I}\{0 \leq \phi < 2.5\} + 3\mathbb{I}\{2.5 \leq \phi < 10\}].$$

756 It can be verified that when  $\alpha = 0.1$ , the optimal solutions of VaR and problem (4) are the same:  
 757

$$z_{\mathcal{U}^*} = z^Q = \begin{cases} 0, & \text{if } x \text{ is 0} \\ 0, & \text{if } x \text{ is 1} \end{cases}.$$

761 For the scenario where decision  $z^Q$  is not equal to decision  $z_{\mathcal{U}^*}$ , consider the following example.  
 762 Let  $\mathcal{X} = \{0, 1\}$  and  $\mathcal{Z} = \{0, 1\}$ . Suppose that the density of  $\phi(Y, z)$  given  $X = x$  is as follows.  
 763

764 For  $x \in \{0, 1\}$ ,  $z = 0$ , the density is  
 765

$$f(\phi) = \frac{1}{15} [1\{\phi \leq 0\} + 2 \sum_{k=1}^2 1\{4k-3 \leq \phi < 4k-1\} + \sum_{k=1}^2 1\{4k-1 \leq \phi < 4k+1\} + 21\{\phi \geq 10\}].$$

771 For  $x \in \{0, 1\}$ ,  $z = 1$ , the density is  
 772

$$f(\phi) = \frac{1}{15} [21\{\phi \leq 0\} + \sum_{k=1}^2 1\{4k-3 \leq \phi < 4k-1\} + 2 \sum_{k=1}^2 1\{4k-1 \leq \phi < 4k+1\} + 1\{\phi \geq 10\}].$$

778 It can be verified that when  $\alpha = 0.4 - 4\epsilon/30$  ( $\epsilon$  is sufficiently small), we have  
 779

$$z^Q = \begin{cases} 0, & \text{if } x \text{ is 0} \\ 0, & \text{if } x \text{ is 1} \end{cases}.$$

782 On the contrary, the solution of the problem (4) is different  
 783

$$z_{\mathcal{U}^*} = \begin{cases} 0, & \text{if } x \text{ is 0} \\ 1, & \text{if } x \text{ is 1} \end{cases}, \quad \mathcal{U}^* = \begin{cases} \{y \in \mathcal{Y} : \phi(y, 0) \leq 6.5 + 2\epsilon\}, & \text{if } x \text{ is 0} \\ \{y \in \mathcal{Y} : \phi(y, 1) \leq 5\}, & \text{if } x \text{ is 1} \end{cases}.$$

787 Note that in the example above,  $\mathcal{X}$  and  $\mathcal{Z}$  are discrete spaces. We can naturally extend them to the  
 788 continuous spaces  $[0, 1]$  while keeping the conclusions unchanged. The specific details are omitted  
 789 here.  $\square$

## 790 B.2 RELATIONSHIP BETWEEN CRC AND RA-DPO, RA-CPO IN KIYANI ET AL. (2025)

792 For classification problems, Kiyani et al. (2025) proposed the following RA-DPO framework for the  
 793 optimal decision:  
 794

$$\min_{z(\cdot), r(\cdot)} \mathbb{E}[r(X)] \quad \text{s.t.} \quad \mathbb{P}\{\phi(Y, z(X)) \leq r(X)\} \geq 1 - \alpha. \quad (8)$$

797 This optimization problem can be viewed as a marginal version of the VaR problem. In addition,  
 798 Kiyani et al. (2025) also defined an optimal decision framework based on prediction sets, called  
 799 RA-CPO, as follows:  
 800

$$\min_{\mathcal{U}(\cdot) : \mathcal{X} \rightarrow 2^{\mathcal{Y}}} \mathbb{E}[r_{\mathcal{U}}(X)] \quad \text{s.t.} \quad \mathbb{P}\{Y \in \mathcal{U}(X)\} \geq 1 - \alpha. \quad (9)$$

802 The difference between RA-CPO and CRC lies in the fact that the former employs a coverage con-  
 803 straint rather than a robustness constraint. We can leverage the idea from Theorem 3.2 in Kiyani et al.  
 804 (2025) to prove the equivalence between the CRC problem and the RA-DPO, RA-CPO problem.  
 805

806 *Proof of Theorem 3.1.* Since RA-DPO and RA-CPO have been proved to be equivalent in Kiyani  
 807 et al. (2025), it suffices to establish the equivalence between RA-DPO and CRC.

808 Let  $(z^{\text{RA-DPO}}(x), r^{\text{RA-DPO}}(x))$  be an optimal solution to RA-DPO. Define the uncertainty set  
 809

$$\mathcal{U}^*(x) = \{y : \phi(y, z^{\text{RA-DPO}}(x)) \leq r^{\text{RA-DPO}}(x)\}.$$

810 Then,

$$\begin{aligned} 812 \quad & \mathbb{P}\{\phi(Y, z_{\mathcal{U}^*}(X)) \leq r_{\mathcal{U}^*}(X)\} \\ 813 \quad & \geq \mathbb{P}\{Y \in \mathcal{U}^*(X)\} \\ 814 \quad & \geq \mathbb{P}\{\phi(Y, z^{\text{RA-DPO}}(X)) \leq r^{\text{RA-DPO}}(X)\} \geq 1 - \alpha. \\ 815 \end{aligned}$$

816 Thus,  $\mathcal{U}^*$  satisfies the constraint of CRC. Moreover, by definition,

$$\begin{aligned} 817 \quad & r_{\mathcal{U}^*}(x) = \arg \min_{z \in \mathcal{Z}} \max_{y \in \mathcal{U}^*(x)} \phi(y, z) \\ 818 \quad & \leq \max_{y \in \mathcal{U}^*(x)} \phi(y, z^{\text{RA-DPO}}(x)) \leq r^{\text{RA-DPO}}(x). \\ 820 \end{aligned}$$

821 Hence,

$$\mathbb{E}[r_{\mathcal{U}^*}(X)] \leq \mathbb{E}[r^{\text{RA-DPO}}(X)].$$

823 This shows that any optimal solution of RA-DPO induces a feasible solution to CRC with a risk  
824 certificate at least as good. Conversely, let  $\mathcal{U}^*$  be an optimal solution to CRC. Define

$$z^{\text{RA-DPO}}(x) = z_{\mathcal{U}^*}(x), \quad r^{\text{RA-DPO}}(x) = r_{\mathcal{U}^*}(x).$$

827 This pair is feasible for RA-DPO and satisfies  $\mathbb{E}[r^{\text{RA-DPO}}(X)] = \mathbb{E}[r_{\mathcal{U}^*}(X)]$ . Therefore, RA-DPO  
828 and CRC are equivalent, and the theorem follows.  $\square$

### 830 B.3 SUPERIORITY OF PARAMETRIZED CRC OVER PARAMETRIZED RA-CPO

832 The parametric formulation of RA-CPO in (9) is given by:

$$\min_{\theta \in \Theta} \mathbb{E}[r_{\theta}(X)] \quad \text{s.t.} \quad \mathbb{P}\{Y \in \mathcal{U}_{\theta}(X)\} \geq 1 - \alpha.$$

835 The difference between parametrized RA-CPO and parametrized CRC (5) lies in the fact that the  
836 former employs a coverage constraint rather than a robustness constraint. The relationship between  
837 the two frameworks is formalized in the following proposition.

838 **Proposition B.2.** *For any parameterized prediction set  $\mathcal{U}_{\theta}(\cdot)$ , it holds that*

$$\mathbb{E}[r_{\theta^{\text{CRC}}}(X)] \leq \mathbb{E}[r_{\theta^{\text{RA-CPO}}}(X)],$$

840 where  $\theta^{\text{CRC}}$  and  $\theta^{\text{RA-CPO}}$  denote the theoretical optimal solutions of the parametrized CRC and  
841 parametrized RA-CPO problems, respectively. Moreover, there exist cases in which the inequality is  
842 strict.

844 In fact, if no constraints are imposed on the prediction set, then as proven in Section B.2, the RA-  
845 CPO and CRC frameworks are equivalent. However, in regression settings, prediction sets are gen-  
846 erally required to satisfy certain structural properties—such as convexity and boundedness—in ad-  
847 dition to being parameterized to render the problem tractable. As a consequence, once the prediction  
848 set is parameterized, the solution derived from the CRC problem typically outperforms that obtained  
849 via RA-CPO.

850 *Proof.* We first show that  $\mathbb{E}[r_{\theta^{\text{CRC}}}(X)] \leq \mathbb{E}[r_{\theta^{\text{RA-CPO}}}(X)]$ . Let  $\mathcal{U}_{\theta^{\text{RA-CPO}}}$  be the optimal solution  
851 to the RA-CPO problem. Since it also satisfies the constraints of the CRC problem, the inequality  
852 follows directly from the definition of the CRC problem.

854 We now proceed to construct a case where the inequality is strict. Consider a parameterized predic-  
855 tion set of the form:

$$856 \quad \mathcal{U}_{\theta}(x) = \{y \in \mathbb{R}^q : (y - \mu(x))^{\top} \Sigma^{-1}(x)(y - \mu(x)) \leq \theta\}, \theta \in \mathbb{R}^+,$$

858 where  $Y | X \sim N(\mu(X), \Sigma(X))$ . Let the loss function be  $\phi(y, z) = -y^{\top} z$ . Then the coverage  
859 probability is given by:

$$860 \quad \mathbb{P}\{Y \in \mathcal{U}_{\theta}(X)\} = \mathbb{P}\{\chi_q^2 \leq \theta\},$$

861 where  $\chi_q^2$  denotes a chi-squared random variable with  $q$  degrees of freedom. To analyze the robust-  
862 ness constraint, we derive the dual of the inner maximization in the CPO problem:

$$863 \quad \max_{y \in \mathcal{U}_{\theta}(X)} -y^{\top} z_{\theta}(X) = \sqrt{\theta} \|\Sigma^{1/2}(X) z_{\theta}(X)\|_2 - \mu(X)^{\top} z_{\theta}(X).$$

864 By the definition of the robustness level, we have:

$$\begin{aligned}
 866 \quad & \mathbb{P} \left\{ \phi(Y, z_\theta(X)) \leq \max_{y \in \mathcal{U}_\theta(X)} \phi(y, z_\theta(X)) \right\} \\
 867 \quad & = \mathbb{P} \left\{ -Y^\top z_\theta(X) \leq \sqrt{\theta} \|\Sigma^{1/2}(X)z_\theta(X)\|_2 - \mu(X)^\top z_\theta(X) \right\} \\
 868 \quad & = \mathbb{P} \left\{ -z_\theta(X)^\top (Y - \mu(X)) \leq \sqrt{\theta} \|\Sigma^{1/2}(X)z_\theta(X)\|_2 \right\} \\
 869 \quad & = \mathbb{P} \left\{ \frac{-z_\theta(X)^\top (Y - \mu(X))}{\|\Sigma^{1/2}(X)z_\theta(X)\|_2} \leq \sqrt{\theta} \right\} = \mathbb{P}\{N(0, 1) \leq \sqrt{\theta}\}.
 \end{aligned}$$

870 Therefore, when  $q \geq 1$ , we obtain:

$$871 \quad \theta^{\text{CRC}} = \Phi_{1-\alpha}^2 < \chi_{q,1-\alpha}^2 = \theta^{\text{RA-CPO}},$$

872 where  $\chi_{q,1-\alpha}^2$  and  $\Phi_{1-\alpha}$  denote the  $(1 - \alpha)$ -quantiles of the  $\chi_q^2$  and  $N(0, 1)$  distributions, respectively. In this case, it follows that:

$$873 \quad \mathbb{E}[r_{\theta^{\text{CRC}}}(X)] < \mathbb{E}[r_{\theta^{\text{RA-CPO}}}(X)],$$

874 which completes the proof.  $\square$

#### 875 B.4 IMPLEMENTATION OF CAL-CRC

---

##### 876 **Algorithm 3** Discretization construction of Cal-CRC

---

877 1: **Input:** Same as Algorithm 2. Discretized space  $\tilde{\mathcal{Y}}$  with finite cardinality. Discretization map-  
 878 ping  $\mathcal{A}(\cdot) : \mathcal{Y} \rightarrow \tilde{\mathcal{Y}}$ . Step size  $\tau_0 > 0$ .

879 2: **Discretization:** Obtain the discretized calibration set  $\tilde{\mathcal{D}}_{\text{cal}} = \{(X_i, \tilde{Y}_i)\}_{i=n_0+1}^n$  by discretiza-  
 880 tion mapping  $\mathcal{A}$ .

881 3: **Calibration initialization:**  $\tilde{\mathcal{U}}_{\text{Cal}}(X_{n+1}) \leftarrow \emptyset$ .

882 4: **for**  $y \in \tilde{\mathcal{Y}}$  **do**

883 5:     Define the augmented calibration set  $\{(X_i, \tilde{Y}_i^y)\}_{i=n_0+1}^{n+1}$ .

884 6:      $t \leftarrow 0$ .

885 7:      $s \leftarrow \frac{1}{n-n_0+1} \sum_{i=n_0+1}^{n+1} \mathbb{1} \left\{ \phi \left( \tilde{Y}_i^y, z_{\hat{\theta}_0, t}(X_i) \right) \leq r_{\hat{\theta}_0, t}(X_i) \right\}$ .

886 8:     **while**  $s < 1 - \alpha$  **do**

887 9:          $t \leftarrow t + \tau_0$ .

888 10:         $s \leftarrow \frac{1}{n-n_0+1} \sum_{i=n_0+1}^{n+1} \mathbb{1} \left\{ \phi \left( \tilde{Y}_i^y, z_{\hat{\theta}_0, t}(X_i) \right) \leq r_{\hat{\theta}_0, t}(X_i) \right\}$ .

889 11:     **end while**

890 12:      $\hat{t}^y \leftarrow t$ .

891 13:     **if**  $\phi \left( y, z_{\hat{\theta}_0, \hat{t}^y}(X_{n+1}) \right) \leq r_{\hat{\theta}_0, \hat{t}^y}(X_{n+1})$  **then**

892 14:          $\tilde{\mathcal{U}}_{\text{Cal}}(X_{n+1}) \leftarrow \tilde{\mathcal{U}}_{\text{Cal}}(X_{n+1}) \cup \{y\}$ .

893 15:     **end if**

894 16: **end for**

895 17: **Anti-discretization:**  $\mathcal{U}_{\text{Cal}}(X_{n+1}) \leftarrow \mathcal{A}^{-1}(\tilde{\mathcal{U}}_{\text{Cal}}(X_{n+1}))$ .

896 18: **Output:**  $\mathcal{U}_{\text{Cal}}(X_{n+1})$ .

---

#### 910 B.5 OPTIMALITY ANALYSIS OF CAL-CRC

911 Under certain conditions, the discrepancy between  $r_{\mathcal{U}_{\text{Cal}}}(X_{n+1})$  and  $r_{\mathcal{U}_{\hat{\theta}_0}}(X_{n+1})$  is expected to  
 912 be negligible. For instance, if  $\hat{t}^y = 0$  for any  $y \in \mathcal{Y}$ , then by the definition of  $\mathcal{U}_{\text{Cal}}$ , we have  
 913  $\mathcal{U}_{\hat{\theta}_0}(X_{n+1}) \subset \mathcal{U}_{\text{Cal}}(X_{n+1})$ . Consequently,

$$914 \quad \max_{y \in \mathcal{U}_{\text{Cal}}(X_{n+1})} \phi(y, z_{\mathcal{U}_{\text{Cal}}}(X_{n+1})) \stackrel{(a)}{\geq} \max_{y \in \mathcal{U}_{\hat{\theta}_0}(X_{n+1})} \phi(y, z_{\mathcal{U}_{\text{Cal}}}(X_{n+1})) \stackrel{(b)}{\geq} \max_{y \in \mathcal{U}_{\hat{\theta}_0}(X_{n+1})} \phi(y, z_{\mathcal{U}_{\hat{\theta}_0}}(X_{n+1})),$$

918 where (a) follows from the inclusion relationship between the two prediction sets, (b) holds due to  
 919 the optimality of  $z_{\mathcal{U}_{\hat{\theta}_0}}(X_{n+1})$  over  $\mathcal{U}_{\hat{\theta}_0}(X_{n+1})$ . On the other hand, from a different perspective,  
 920

$$921 \max_{y \in \mathcal{U}_{\text{Cal}}(X_{n+1})} \phi(y, z_{\mathcal{U}_{\text{Cal}}}(X_{n+1})) \stackrel{(c)}{\leq} \max_{y \in \mathcal{U}_{\text{Cal}}(X_{n+1})} \phi(y, z_{\mathcal{U}_{\hat{\theta}_0}}(X_{n+1})) \stackrel{(d)}{\leq} \max_{y \in \mathcal{U}_{\hat{\theta}_0}(X_{n+1})} \phi(y, z_{\mathcal{U}_{\hat{\theta}_0}}(X_{n+1})),$$

924 where (c) is due to the optimality of  $z_{\mathcal{U}_{\text{Cal}}}(X_{n+1})$  over  $\mathcal{U}_{\text{Cal}}$ , and (d) follows from the definition  
 925 of the  $\mathcal{U}_{\text{Cal}}$ . Combining these results yields  $r_{\mathcal{U}_{\hat{\theta}_0}}(X_{n+1}) = r_{\mathcal{U}_{\text{Cal}}}(X_{n+1})$ . We now consider a  
 926 more general setting. First, we state the generalized conditions, and then present the corresponding  
 927 theoretical results.

928 **Condition B.1.** Assume that for all  $y \in \mathcal{Y}$ , we have  $|\hat{t}^y| \leq t_0$ , where  $t_0$  is a positive constant.  
 929

930 **Condition B.2.** Loss function  $\phi$  is  $L_\phi$ -Lipschitz in decision  $z$  for any  $y \in \mathcal{Y}$ . The decision  
 931  $z_{\hat{\theta}_0, t}(X_{n+1})$  is  $L_z$ -Lipschitz in  $t \leq t_0$ . The risk certificate  $r_{\hat{\theta}_0, t}(X_{n+1})$  is  $L_r$ -Lipschitz in  $t \leq t_0$ .

932 **Theorem B.1.** Suppose that  $\hat{\theta}_0$  is obtained by running Algorithm 1 on the training dataset  $\mathcal{D}_{\text{train}}$ .  
 933 Under conditions B.1 and B.2 in the calibration process, the following result holds:

$$935 \quad r_{\mathcal{U}_{\text{Cal}}}(X_{n+1}) \leq r_{\mathcal{U}_{\hat{\theta}_0}}(X_{n+1}) + t_0(L_\phi L_z + L_r).$$

937 *Proof.* For any  $y \in \mathcal{U}_{\text{Cal}}(X_{n+1})$ , we have

$$939 \quad \begin{aligned} \phi(y, z_{\hat{\theta}_0}(X_{n+1})) &\leq \phi(y, z_{\hat{\theta}_0, \hat{t}^y}(X_{n+1})) + t_0 L_\phi L_z \\ 940 &\leq r_{\hat{\theta}_0, \hat{t}^y}(X_{n+1}) + t_0 L_\phi L_z \\ 941 &\leq r_{\mathcal{U}_{\hat{\theta}_0}}(X_{n+1}) + t_0(L_\phi L_z + L_r). \end{aligned}$$

943 Therefore,

$$945 \quad \begin{aligned} \max_{y \in \mathcal{U}_{\text{Cal}}(X_{n+1})} \phi(y, z_{\text{Cal}}(X_{n+1})) &\leq \max_{y \in \mathcal{U}_{\text{Cal}}(X_{n+1})} \phi(y, z_{\hat{\theta}_0}(X_{n+1})) \\ 946 &\leq r_{\mathcal{U}_{\hat{\theta}_0}}(X_{n+1}) + t_0(L_\phi L_z + L_r). \end{aligned}$$

948  $\square$

951 Note that  $r_{\hat{\theta}_0, t}(x)$  is monotonically increasing in  $t$  for any  $x \in \mathcal{X}$ . Hence, if the initial model  $\mathcal{U}_{\hat{\theta}_0}$   
 952 already approximately satisfies the  $1 - \alpha$  robustness requirement, the calibrated threshold  $\hat{t}^y$  will  
 953 generally remain small for all  $y \in \mathcal{Y}$ . As a result,  $\mathcal{U}_{\text{Cal}}$  can maintain risk certificates and decision  
 954 losses comparable to those of the initial model  $\mathcal{U}_{\hat{\theta}_0}$ . Conversely, if the initial model's robustness  
 955 is significantly below  $1 - \alpha$ , then although  $\mathcal{U}_{\text{Cal}}$  still guarantee  $1 - \alpha$  robustness, it may produce  
 956 relatively conservative results.

## 958 C PROOF OF MAIN RESULTS IN SECTION 3.3

### 959 C.1 PROOF OF THEOREM 3.2

962 By leveraging the finite covering property of the function class and large-sample probability in-  
 963 equalities, we aim to prove that the empirical estimates converge uniformly to their expected values,  
 964 thereby establishing the conclusion of the theorem. First, given an  $\epsilon_{2n}$ -covering  $\Theta_{\epsilon_{2n}}$  with smallest  
 965 cardinality of the function class, and applying the Dvoretzky-Kiefer-Wolfowitz (DKW) inequality  
 966 (Massart, 1990), we have

$$967 \quad \mathbb{P} \left\{ \sup_{t \in \mathbb{R}, \theta_0 \in \Theta_{\epsilon_{2n}}} \left| \frac{1}{n} \sum_{i=1}^n \mathbb{1} \{ V_{\theta_0}(X_i, Y_i) \leq t \} - \mathbb{P} \{ V_{\theta_0}(X, Y) \leq t \} \right| \geq \epsilon_{1n} \right\} \leq 2\mathcal{N}(\Theta, \|\cdot\|_\infty, \epsilon_{2n}) e^{-2n\epsilon_{1n}^2},$$

971 where  $\epsilon_{1n}$  is the tolerance error, whose specific value will depend on the covering number  $\mathcal{N}(\Theta, \|\cdot\|_\infty, \epsilon_{2n})$  and will be specified later. According to the definition of  $\epsilon_{2n}$ -covering, for any given

$\theta \in \Theta$ , there exists  $\theta_0 \in \Theta_{\epsilon_{2n}}$  such that  $\|\theta - \theta_0\| \leq \epsilon_{2n}$ . Therefore, the upper bound on the deviation between the empirical estimate and the expected value can be derived as follows:

$$\begin{aligned} & \left| \frac{1}{n} \sum_{i=1}^n \mathbb{1}\{V_\theta(X_i, Y_i) \leq 0\} - \mathbb{P}\{V_\theta(X, Y) \leq 0\} \right| \\ & \leq \left| \frac{1}{n} \sum_{i=1}^n \mathbb{1}\{V_\theta(X_i, Y_i) \leq 0\} - \frac{1}{n} \sum_{i=1}^n \mathbb{1}\{V_{\theta_0}(X_i, Y_i) \leq 0\} \right| \end{aligned} \quad (10)$$

$$\begin{aligned} & + \left| \frac{1}{n} \sum_{i=1}^n \mathbb{1}\{V_{\theta_0}(X_i, Y_i) \leq 0\} - \mathbb{P}\{V_{\theta_0}(X, Y) \leq 0\} \right| \\ & + |\mathbb{P}\{V_{\theta_0}(X, Y) \leq 0\} - \mathbb{P}\{V_\theta(X, Y) \leq 0\}|. \end{aligned} \quad (11)$$

Leveraging the Lipschitz condition, (10) and (11) can be bounded as follows:

$$\begin{aligned} & \left| \frac{1}{n} \sum_{i=1}^n \mathbb{1}\{V_\theta(X_i, Y_i) \leq 0\} - \frac{1}{n} \sum_{i=1}^n \mathbb{1}\{V_{\theta_0}(X_i, Y_i) \leq 0\} \right| \\ & \leq \left| \frac{1}{n} \sum_{i=1}^n \mathbb{1}\{V_{\theta_0}(X_i, Y_i) \leq (L_\phi L_z + L_r)\|\theta - \theta_0\|\} - \frac{1}{n} \sum_{i=1}^n \mathbb{1}\{V_{\theta_0}(X_i, Y_i) \leq 0\} \right| \\ & + \left| \frac{1}{n} \sum_{i=1}^n \mathbb{1}\{V_{\theta_0}(X_i, Y_i) \leq -(L_\phi L_z + L_r)\|\theta - \theta_0\|\} - \frac{1}{n} \sum_{i=1}^n \mathbb{1}\{V_{\theta_0}(X_i, Y_i) \leq 0\} \right| \\ & \leq 4 \sup_{t \in \mathbb{R}, \theta_0 \in \Theta_{\epsilon_{2n}}} \left| \frac{1}{n} \sum_{i=1}^n \mathbb{1}\{V_{\theta_0}(X_i, Y_i) \leq t\} - \mathbb{P}\{V_{\theta_0}(X, Y) \leq t\} \right| \\ & + \sup_{\theta_0 \in \Theta_{\epsilon_{2n}}} \mathbb{P}\{-(L_\phi L_z + L_r)\epsilon_{2n} \leq V_{\theta_0}(X, Y) \leq (L_\phi L_z + L_r)\epsilon_{2n}\}, \end{aligned}$$

and

$$\begin{aligned} & |\mathbb{P}\{V_{\theta_0}(X, Y) \leq 0\} - \mathbb{P}\{V_\theta(X, Y) \leq 0\}| \\ & \leq |\mathbb{P}\{V_{\theta_0}(X, Y) \leq 0\} - \mathbb{P}\{V_{\theta_0}(X, Y) \leq (L_\phi L_z + L_r)\|\theta_0 - \theta\|\}| \\ & + |\mathbb{P}\{V_{\theta_0}(X, Y) \leq 0\} - \mathbb{P}\{V_{\theta_0}(X, Y) \leq -(L_\phi L_z + L_r)\|\theta_0 - \theta\|\}| \\ & \leq \sup_{\theta_0 \in \Theta_{\epsilon_{2n}}} \mathbb{P}\{-(L_\phi L_z + L_r)\epsilon_{2n} \leq V_{\theta_0}(X, Y) \leq (L_\phi L_z + L_r)\epsilon_{2n}\}. \end{aligned}$$

Finally, we consolidate the above results and obtain

$$\begin{aligned} & \left| \frac{1}{n} \sum_{i=1}^n \mathbb{1}\{V_\theta(X_i, Y_i) \leq 0\} - \mathbb{P}\{V_\theta(X, Y) \leq 0\} \right| \\ & \leq 5 \sup_{t \in \mathbb{R}, \theta_0 \in \Theta_{\epsilon_{2n}}} \left| \frac{1}{n} \sum_{i=1}^n \mathbb{1}\{V_{\theta_0}(X_i, Y_i) \leq t\} - \mathbb{P}\{V_{\theta_0}(X, Y) \leq t\} \right| \\ & + 2 \sup_{\theta_0 \in \Theta_{\epsilon_{2n}}} \mathbb{P}\{-(L_\phi L_z + L_r)\epsilon_{2n} \leq V_{\theta_0}(X, Y) \leq (L_\phi L_z + L_r)\epsilon_{2n}\}. \end{aligned}$$

Let  $\epsilon_{1n} = \sqrt{\frac{\log(2\mathcal{N}(\Theta, \|\cdot\|_\infty, \epsilon_{2n})) + \log(1/\delta)}{2n}}$ . We have

$$\begin{aligned} \sup_{\theta \in \Theta} \left| \frac{1}{n} \sum_{i=1}^n \mathbb{1}\{V_\theta(X_i, Y_i) \leq 0\} - \mathbb{P}\{V_\theta(X, Y) \leq 0\} \right| & \leq 5 \sqrt{\frac{\log(2\mathcal{N}(\Theta, \|\cdot\|_\infty, \epsilon_{2n})) + \log(1/\delta)}{2n}} \\ & + 4(L_\phi L_z + L_r)\rho_0 \epsilon_{2n}, \end{aligned} \quad (12)$$

with probability at least  $1 - \delta$ . Furthermore, we have, with probability at least  $1 - \delta$ ,

$$\begin{aligned} \mathbb{P}\{\phi(Y, z_{\hat{\theta}}(X)) \leq r_{\hat{\theta}}(X) \mid \mathcal{D}_n\} & \geq 1 - \alpha - 5 \sqrt{\frac{\log(2\mathcal{N}(\Theta, \|\cdot\|_\infty, \epsilon_{2n})) + \log(1/\delta)}{2n}} \\ & - 4(L_\phi L_z + L_r)\rho_0 \epsilon_{2n}, \end{aligned}$$

where  $\hat{\theta}$  is the solution to the CRC problem on dataset  $\mathcal{D}_n$ .

1026 C.2 PROOF OF THEOREM 3.3  
1027

1028 Let  $\theta^*$  be the convenient notation of  $\theta_{\Delta_n}^*$ . The following formula gives the risk difference between  
1029 the estimated model  $\hat{\theta}$  and the optimal model  $\theta^*$ :

$$1031 \mathbb{E}[r_{\hat{\theta}}(X) | \mathcal{D}_n] - \mathbb{E}[r_{\theta^*}(X)] \leq \left| \mathbb{E}[r_{\hat{\theta}}(X) | \mathcal{D}_n] - \frac{1}{n} \sum_{i=1}^n r_{\hat{\theta}}(X_i) \right| \quad (13)$$

$$1034 + \frac{1}{n} \sum_{i=1}^n r_{\hat{\theta}}(X_i) - \frac{1}{n} \sum_{i=1}^n r_{\theta^*}(X_i) \quad (14)$$

$$1037 + \left| \frac{1}{n} \sum_{i=1}^n r_{\theta^*}(X_i) - \mathbb{E}[r_{\theta^*}(X)] \right| \quad (15)$$

1040 For formulas (13) and (15), we adopt a proof strategy similar to that of Theorem 3.2 to demonstrate  
1041 that the empirical estimates converge uniformly to their expected value. Given  $\theta \in \Theta$ , let  $\theta_0 \in \Theta_{\epsilon_{2n}}$   
1042 be the approximation of  $\theta$  in  $\epsilon_{2n}$ -covering  $\Theta_{\epsilon_{2n}}$ . We have

$$1043 \left| \frac{1}{n} \sum_{i=1}^n r_{\theta}(X_i) - \mathbb{E}[r_{\theta}(X)] \right| \leq \left| \frac{1}{n} \sum_{i=1}^n r_{\theta}(X_i) - \frac{1}{n} \sum_{i=1}^n r_{\theta_0}(X_i) \right| \\ 1044 + \left| \frac{1}{n} \sum_{i=1}^n r_{\theta_0}(X_i) - \mathbb{E}[r_{\theta_0}(X)] \right| \\ 1045 + |\mathbb{E}[r_{\theta_0}(X)] - \mathbb{E}[r_{\theta}(X)]| \\ 1046 \leq \sup_{\theta_0 \in \Theta_{\epsilon_{2n}}} \left| \frac{1}{n} \sum_{i=1}^n r_{\theta_0}(X_i) - \mathbb{E}[r_{\theta_0}(X)] \right| \\ 1047 + 2L_r \epsilon_{2n},$$

1048 where the last term is derived by applying the Lipschitz condition. According to Hoeffding's in-  
1049 equality, we have:

$$1057 \sup_{\theta_0 \in \Theta_{\epsilon_{2n}}} \left| \frac{1}{n} \sum_{i=1}^n r_{\theta_0}(X_i) - \mathbb{E}[r_{\theta_0}(X)] \right| \leq 2B_r \sqrt{\frac{\log(2\mathcal{N}(\Theta, \|\cdot\|_{\infty}, \epsilon_{2n}) + \log(1/\delta)}{2n}},$$

1058 with probability at least  $1 - \delta$ . Furthermore, we can derive upper bounds for formulas (13) and (15).  
1059 For formula (14), we assume that event (12) in the proof of Theorem 3.2 holds. At this point, since  
1060  $\hat{\theta}$  is the solution to the finite-sample CRC problem, we deduce the following result:

$$1064 \frac{1}{n} \sum_{i=1}^n r_{\hat{\theta}}(X_i) - \frac{1}{n} \sum_{i=1}^n r_{\theta^*}(X_i) \leq 0.$$

1065 Integrating the above conclusions, we can obtain the following result:

$$1069 \mathbb{E}[r_{\hat{\theta}}(X) | \mathcal{D}_n] - \mathbb{E}[r_{\theta^*}(X)] \leq 4B_r \sqrt{\frac{\log(2\mathcal{N}(\Theta, \|\cdot\|_{\infty}, \epsilon_{2n}) + \log(1/\delta)}{2n}} + 4L_r \epsilon_{2n}.$$

1070 holds with probability at least  $1 - 2\delta$ .

## 1073 C.3 PROOF OF THEOREM 4.1

1075 Suppose that the calibration set is  $\mathcal{D}_{\text{cal}} = \{(X_i, Y_i)\}_{i=n_0+1}^n$ , the test data is  $(X_{n+1}, Y_{n+1})$  and a  
1076 model  $\hat{\theta}_0$  has been trained from the training set  $\mathcal{D}_{\text{train}} = \{(X_i, Y_i)\}_{i=1}^{n_0}$ . First, we demonstrate that  
1077 the prediction set  $\mathcal{U}_{\text{Cal}}(\cdot)$  achieves  $1 - \alpha$  coverage. Note that

$$1079 \mathbb{P}\{Y_{n+1} \in \mathcal{U}_{\text{Cal}}(X_{n+1})\} = \mathbb{P}\left\{\phi\left(Y_{n+1}, z_{\hat{\theta}_0, \hat{t}^{Y_{n+1}}}(X_{n+1})\right) \leq r_{\hat{\theta}_0, \hat{t}^{Y_{n+1}}}(X_{n+1})\right\}.$$

1080 Let  $W = \{(X_{n_0+1}, Y_{n_0+1}), \dots, (X_{n+1}, Y_{n+1})\}$  be an unordered set. Note that  $\hat{t}^{Y_{n+1}}$  is measurable  
 1081 with respect to statistic  $W$ . We will complete the proof by leveraging the symmetry of the data.  
 1082

$$\begin{aligned} 1083 \quad & \mathbb{P} \left\{ \phi \left( Y_{n+1}, z_{\hat{\theta}_0, \hat{t}^{Y_{n+1}}} (X_{n+1}) \right) \leq r_{\hat{\theta}_0, \hat{t}^{Y_{n+1}}} (X_{n+1}) \right\} \\ 1084 \quad & = \mathbb{E} \left[ \mathbb{E} \left[ \mathbb{1} \left\{ \phi \left( Y_{n+1}, z_{\hat{\theta}_0, \hat{t}^{Y_{n+1}}} (X_{n+1}) \right) \leq r_{\hat{\theta}_0, \hat{t}^{Y_{n+1}}} (X_{n+1}) \right\} \mid W \right] \right] \\ 1085 \quad & = \mathbb{E} \left[ \frac{1}{n - n_0 + 1} \sum_{i=n_0+1}^{n+1} \mathbb{1} \left\{ \phi \left( Y_i, z_{\hat{\theta}_0, \hat{t}^{Y_{n+1}}} (X_i) \right) \leq r_{\hat{\theta}_0, \hat{t}^{Y_{n+1}}} (X_i) \right\} \right] \\ 1086 \quad & \geq 1 - \alpha. \\ 1087 \end{aligned}$$

1091 The first equality stems from the law of total expectation. The second equality arises from the  
 1092 symmetry of the data, a technique frequently employed in proofs within conformal prediction meth-  
 1093 ods (Vovk et al., 2005; Liang et al., 2024). The final inequality is derived from the definition of  
 1094 threshold  $\hat{t}^{Y_{n+1}}$ , as referenced in Algorithm 2. Finally, since the coverage constraint is a sufficient  
 1095 condition for the robustness constraint, we can obtain the robustness guarantee, i.e.,  
 1096

$$\mathbb{P} \{ \phi (Y_{n+1}, z_{\mathcal{U}_{\text{Cal}}}(X_{n+1})) \leq r_{\mathcal{U}_{\text{Cal}}}(X_{n+1}) \} \geq \mathbb{P} \{ Y_{n+1} \in \mathcal{U}_{\text{Cal}}(X_{n+1}) \} \geq 1 - \alpha.$$

## D ADDITIONAL THEORETICAL RESULTS

### D.1 THEORETICAL RESULTS FOR VC/RADEMACHER CLASS

1102 In this section, we present theoretical results on robustness and optimality when the function class  
 1103 has a finite VC dimension. Additionally, we discuss a decision-making method based on parti-  
 1104 tioning the covariate domain (Chenreddy et al., 2022). Under this approach, the corresponding  
 1105 function class possesses a finite VC dimension, thereby exhibiting relevant convergence properties.  
 1106 Let  $\text{VC}(\mathcal{C}) := \text{VC}(\{(x, y) \rightarrow \mathbb{1} \{ \phi(y, z_\theta(x)) \leq r_\theta(x) \} : \theta \in \Theta\})$  denote the VC dimension of the  
 1107 robustness-induced classifier class.

1108 **Theorem D.1** (VC class robustness). *Suppose  $\text{VC}(\mathcal{C}) = H < \infty$ . Then there exists an absolute  
 1109 constant  $C > 0$  such that, with probability at least  $1 - \delta$ ,*

$$1111 \quad \mathbb{P} \{ \phi (Y, z_{\hat{\theta}}(X)) \leq r_{\hat{\theta}}(X) \mid \mathcal{D}_n \} \geq 1 - \alpha - C \sqrt{\frac{H}{n}} - \sqrt{\frac{\log(2/\delta)}{2n}}.$$

1114 *Proof.* By McDiarmid's Inequality, with probability at least  $1 - \delta$ ,

$$\begin{aligned} 1116 \quad & \sup_{\theta \in \Theta} \left| \frac{1}{n} \sum_{i=1}^n \mathbb{1} \{ \phi (Y_i, z_\theta(X_i)) \leq r_\theta(X_i) \} - \mathbb{P} \{ \phi (Y, z_\theta(X)) \leq r_\theta(X) \} \right| \\ 1117 \quad & \leq \mathbb{E} \left[ \sup_{\theta \in \Theta} \left| \frac{1}{n} \sum_{i=1}^n \mathbb{1} \{ \phi (Y_i, z_\theta(X_i)) \leq r_\theta(X_i) \} - \mathbb{P} \{ \phi (Y, z_\theta(X)) \leq r_\theta(X) \} \right| \right] \quad (16) \\ 1118 \quad & + \sqrt{\frac{\log(2/\delta)}{2n}}. \\ 1119 \end{aligned}$$

1124 The expectation in (16) can be bounded using the standard VC-class Rademacher bounds (Ver-  
 1125 shynin, 2018, Theorem 8.3.23): there exists a constant  $C$  such that

$$1126 \quad \mathbb{E} \left[ \sup_{\theta \in \Theta} \left| \frac{1}{n} \sum_{i=1}^n \mathbb{1} \{ \phi (Y_i, z_\theta(X_i)) \leq r_\theta(X_i) \} - \mathbb{P} \{ \phi (Y, z_\theta(X)) \leq r_\theta(X) \} \right| \right] \leq C \sqrt{\frac{H}{n}}.$$

1129 Combining these results yields that, with probability at least  $1 - \delta$ :

$$1131 \quad \mathbb{P} \{ \phi (Y, z_{\hat{\theta}}(X)) \leq r_{\hat{\theta}}(X) \mid \mathcal{D}_n \} \geq 1 - \alpha - C \sqrt{\frac{H}{n}} - \sqrt{\frac{\log(2/\delta)}{2n}}.$$

□

1134 **Theorem D.2** (Rademacher risk). *Assume additionally that  $|r_\theta(x)| \leq M$  for all  $\theta \in \Theta$  and  $x \in \mathcal{X}$ .  
1135 Let  $\theta_{\Delta_n}^*$  be the optimal solution of problem (5) at robustness level  $1 - \alpha + \Delta_n$  where  $\Delta_n = C\sqrt{\frac{H}{n}} +$   
1136  $\sqrt{\frac{\log(2/\delta)}{2n}}$ . Then, with probability at least  $1 - 2\delta$ ,*

$$1139 \mathbb{E} [r_{\hat{\theta}}(X) - r_{\theta^*}(X) \mid \mathcal{D}_n] \leq 4\mathcal{R}_n(\{r_\theta(\cdot) : \theta \in \Theta\}) + 2M\sqrt{\frac{\log(4/\delta)}{2n}},$$

1140 where  $\mathcal{R}_n(\{r_\theta(\cdot) : \theta \in \Theta\})$  denotes the Rademacher complexity for function class  $\{r_\theta(\cdot) : \theta \in \Theta\}$ .

1141 *Proof.* Let  $\theta^* = \theta_{\Delta_n}^*$ . We bound the risk difference between the estimated model  $\hat{\theta}$  and the optimal  
1142 model  $\theta^*$  as follows:

$$1143 \mathbb{E} [r_{\hat{\theta}}(X) \mid \mathcal{D}_n] - \mathbb{E} [r_{\theta^*}(X)] \leq \left| \mathbb{E}[r_{\hat{\theta}}(X) \mid \mathcal{D}_n] - \frac{1}{n} \sum_{i=1}^n r_{\hat{\theta}}(X_i) \right| \\ 1144 + \frac{1}{n} \sum_{i=1}^n r_{\hat{\theta}}(X_i) - \frac{1}{n} \sum_{i=1}^n r_{\theta^*}(X_i) \\ 1145 + \left| \frac{1}{n} \sum_{i=1}^n r_{\theta^*}(X_i) - \mathbb{E}[r_{\theta^*}(X)] \right| \\ 1146 \leq 2 \sup_{\theta \in \Theta} \left| \frac{1}{n} \sum_{i=1}^n r_\theta(X_i) - \mathbb{E}[r_\theta(X)] \right| \quad (17)$$

$$1147 + \frac{1}{n} \sum_{i=1}^n r_{\hat{\theta}}(X_i) - \frac{1}{n} \sum_{i=1}^n r_{\theta^*}(X_i). \quad (18)$$

1148 For the term (17), by McDiarmid's inequality, with probability  $1 - \delta$ :

$$1149 \sup_{\theta \in \Theta} \left| \frac{1}{n} \sum_{i=1}^n r_\theta(X_i) - \mathbb{E}[r_\theta(X)] \right| \leq \mathbb{E} \left[ \sup_{\theta \in \Theta} \left| \frac{1}{n} \sum_{i=1}^n r_\theta(X_i) - \mathbb{E}[r_\theta(X)] \right| \right] + 2M\sqrt{\frac{\log(2/\delta)}{2n}}. \quad (19)$$

1150 The expectation in (19) is bounded via Rademacher complexity:

$$1151 \mathbb{E} \left[ \sup_{\theta \in \Theta} \left| \frac{1}{n} \sum_{i=1}^n r_\theta(X_i) - \mathbb{E}[r_\theta(X)] \right| \right] \leq 2\mathbb{E} \left[ \sup_{\theta \in \Theta} \left| \frac{1}{n} \sum_{i=1}^n \epsilon_i r_\theta(X_i) \right| \right] = 2\mathcal{R}_n(\{r_\theta(\cdot) : \Theta\}).$$

1152 For the term (18), whenever

$$1153 \left| \frac{1}{n} \sum_{i=1}^n \mathbb{1}\{\phi(Y_i, z_{\theta^*}(X_i)) \leq r_{\theta^*}(X_i)\} - \mathbb{P}\{\phi(Y, z_{\theta^*}(X)) \leq r_{\theta^*}(X)\} \right| \leq C\sqrt{\frac{H}{n}} + \sqrt{\frac{\log(2/\delta)}{2n}}$$

1154 the definition of problem (6) implies

$$1155 \frac{1}{n} \sum_{i=1}^n r_{\hat{\theta}}(X_i) - \frac{1}{n} \sum_{i=1}^n r_{\theta^*}(X_i) \leq 0.$$

1156 By Theorem D.1, this event holds with probability at least  $1 - \delta$ . A union bound gives that, with  
1157 probability at least  $1 - 2\delta$ :

$$1158 \mathbb{E} [r_{\hat{\theta}}(X) \mid \mathcal{D}_n] - \mathbb{E} [r_{\theta^*}(X)] \leq 4\mathcal{R}_n(\{r_\theta(\cdot) : \theta \in \Theta\}) + 2M\sqrt{\frac{\log(2/\delta)}{2n}}.$$

1159  $\square$

1160 **Remark D.1.** In Chenreddy et al. (2022), the authors introduce a decision-making framework that  
1161 leverages data-driven learning of underlying structures to categorize individuals into  $K$  classes  
1162 based on their covariates. For each class, a prediction set is constructed, which in turn induces

1188  
 1189 *specific decisions and risk certificates. Denote the trained classifier by  $\mathcal{A} : \mathcal{X} \rightarrow [K]$  and the model*  
 1190 *parameters by  $\theta$ . The decisions and risk certificates take the following forms:*

$$1191 \quad z_\theta(x) = \sum_{k=1}^K z_\theta^k \mathbb{1}\{\mathcal{A}(x) = k\} \quad r_\theta(x) = \sum_{k=1}^K r_\theta^k \mathbb{1}\{\mathcal{A}(x) = k\},$$

1194  
 1195 *where  $z_k \in \mathcal{Z}, r_k \in \mathbb{R}$  for each  $k \in [K]$ . Considering a portfolio optimization problem with*  
 1196 *loss function  $\phi(y, z) = -y^\top z$  and  $\mathcal{Y} = \mathbb{R}^q$ , the set  $\{(x, y) \rightarrow \mathbb{1}\{\phi(y, z_\theta(x)) \leq r_\theta(x)\} : \theta \in \Theta\}$*   
 1197 *becomes a subset of the following family:*

$$1198 \quad \left\{ (x, y) \rightarrow \mathbb{1} \left\{ \sum_{k=1}^K (a_k^\top y - r_k) \mathbb{1}\{\mathcal{A}(x) = k\} \leq 0 \right\} : a_k \in \mathbb{R}^q, r_k \in \mathbb{R} \text{ for all } k \in [K] \right\}.$$

1201  
 1202 *This family corresponds to a finite-dimensional linear space of functions and therefore has VC di-*  
 1203 *mension at most  $(q+1)K$ . Applying Theorem D.1, we obtain the following convergence guarantee:*  
 1204 *with probability at least  $1 - \delta$ ,*

$$1205 \quad \mathbb{P}\{\phi(Y, z_{\hat{\theta}}(X)) \leq r_{\hat{\theta}}(X) \mid \mathcal{D}_n\} \geq 1 - \alpha - C \sqrt{\frac{(q+1)K}{n}} - \sqrt{\frac{\log(2/\delta)}{2n}},$$

1208  
 1209 *Similarly, the function class  $\{r_\theta(x) : \theta \in \Theta\}$  is uniformly bounded and has VC dimension at most*  
 1210  *$K + 1$ . Hence, its Rademacher complexity satisfies  $\mathcal{R}_n(\{r_\theta : \theta \in \Theta\}) \leq C' \sqrt{\frac{K+1}{n}}$  for some*  
 1211 *constant  $C'$ . This leads to the following bound on the excess risk: with probability at least  $1 - 2\delta$ ,*

$$1213 \quad \mathbb{E}[r_{\hat{\theta}}(X) - r_{\theta^*}(X) \mid \mathcal{D}_n] \leq 4C' \sqrt{\frac{K+1}{n}} + 2M \sqrt{\frac{\log(2/\delta)}{2n}}.$$

1215  
 1216 *It is worth noting that, under the finite VC dimension condition, the resulting convergence rate*  
 1217 *achieves the order  $O(\sqrt{1/n})$ .*

## 1219 D.2 THEORETICAL RESULTS UNDER SMOOTH CONSTRAINT

1221 In this section, we analyze the theoretical properties of the optimal solution to the following  
 1222 smoothed optimization problem:

$$1224 \quad \hat{\theta} = \arg \min_{\theta \in \Theta} \frac{1}{n} \sum_{i=1}^n r_\theta(X_i) \quad \text{s.t.} \quad \frac{1}{n} \sum_{i=1}^n \tilde{\mathbb{1}}\{\phi(Y_i, z_\theta(X_i)) \leq r_\theta(X_i)\} \geq 1 - \alpha. \quad (20)$$

1227 Here,  $\tilde{\mathbb{1}}\{a \leq b\} = \frac{1}{2}(1 + \text{erf}(\frac{b-a}{\sqrt{2}\sigma}))$ , where  $\text{erf}(x) = \frac{2}{\sqrt{\pi}} \int_0^x e^{-t^2} dt$  is the Gaussian error function  
 1228 and  $\sigma$  controls the smoothness of the surrogate. This formulation provides a smoothed approxi-  
 1229 mation of (6) and serves as the direct optimization target in Algorithm 1. The next two theorems  
 1230 provide a non-asymptotic guarantees of the robustness and expected risk certificate value of the  
 1231 resulting solution.

1232 **Theorem D.3 (Robustness).** *Let  $\Theta_\epsilon$  denote an  $\epsilon$ -covering of the  $\Theta$  with coverage number  $\mathcal{N}(\Theta, \|\cdot\|_\infty, \epsilon)$ , and let  $\hat{\theta}$  be the solution of problem (20). Under Conditions 3.1-3.2, for any independent*  
 1233 *data  $(X, Y) \sim P$  and conditioning on the labeled data  $\mathcal{D}_n$ , we have*

$$1237 \quad \mathbb{P}\{\phi(Y, z_{\hat{\theta}}(X)) \leq r_{\hat{\theta}}(X) \mid \mathcal{D}_n\} \geq 1 - \alpha - \sqrt{\frac{\log(2\mathcal{N}(\Theta, \|\cdot\|_\infty, \epsilon) + \log(1/\delta))}{2n}} \\ 1238 \quad - \frac{2(L_z L_\phi + L_r)\epsilon}{\sqrt{2\pi}\sigma} - \sqrt{\frac{\pi}{2}}\sigma\rho_0,$$

1241 *with probability at least  $1 - \delta$ .*

1242 *Proof.* For any  $\theta \in \Theta$ , let  $\theta_0 \in \Theta_\epsilon$  such that  $\|\theta - \theta_0\| < \epsilon$ . We decompose the deviation as follows:  
1243

$$\begin{aligned} 1244 & \left| \frac{1}{n} \sum_{i=1}^n \tilde{\mathbb{1}} \{ \phi(Y_i, z_\theta(X_i)) \leq r_\theta(X_i) \} - \mathbb{E} [\tilde{\mathbb{1}} \{ \phi(Y, z_\theta(X)) \leq r_\theta(X) \}] \right| \\ 1245 & \leq \left| \frac{1}{n} \sum_{i=1}^n \tilde{\mathbb{1}} \{ \phi(Y_i, z_\theta(X_i)) \leq r_\theta(X_i) \} - \frac{1}{n} \sum_{i=1}^n \tilde{\mathbb{1}} \{ \phi(Y_i, z_{\theta_0}(X_i)) \leq r_{\theta_0}(X_i) \} \right| \quad (21) \\ 1246 \end{aligned}$$

$$\begin{aligned} 1247 & + \left| \frac{1}{n} \sum_{i=1}^n \tilde{\mathbb{1}} \{ \phi(Y_i, z_{\theta_0}(X_i)) \leq r_{\theta_0}(X_i) \} - \mathbb{E} [\tilde{\mathbb{1}} \{ \phi(Y, z_{\theta_0}(X)) \leq r_{\theta_0}(X) \}] \right| \quad (22) \\ 1248 & + \left| \mathbb{E} [\tilde{\mathbb{1}} \{ \phi(Y, z_{\theta_0}(X)) \leq r_{\theta_0}(X) \}] - \mathbb{E} [\tilde{\mathbb{1}} \{ \phi(Y, z_\theta(X)) \leq r_\theta(X) \}] \right| \quad (23) \\ 1249 \end{aligned}$$

1250 We can apply the Lipschitz condition to bound term (21):  
1251

$$\begin{aligned} 1252 & \left| \frac{1}{n} \sum_{i=1}^n \tilde{\mathbb{1}} \{ \phi(Y_i, z_\theta(X_i)) \leq r_\theta(X_i) \} - \frac{1}{n} \sum_{i=1}^n \tilde{\mathbb{1}} \{ \phi(Y_i, z_{\theta_0}(X_i)) \leq r_{\theta_0}(X_i) \} \right| \\ 1253 & \leq \frac{1}{n} \sum_{i=1}^n \left| \tilde{\mathbb{1}} \{ \phi(Y_i, z_\theta(X_i)) \leq r_\theta(X_i) \} - \tilde{\mathbb{1}} \{ \phi(Y_i, z_{\theta_0}(X_i)) \leq r_{\theta_0}(X_i) \} \right| \\ 1254 & \stackrel{(a)}{\leq} \frac{1}{n\sigma\sqrt{2\pi}} \sum_{i=1}^n |\phi(Y_i, z_\theta(X_i)) - \phi(Y_i, z_{\theta_0}(X_i))| + |r_\theta(X_i) - r_{\theta_0}(X_i)| \\ 1255 & \stackrel{(b)}{\leq} \frac{(L_z L_\phi + L_r)\epsilon}{\sqrt{2\pi}\sigma}, \\ 1256 \end{aligned}$$

1257 where (a) is due to the fact that function  $\mathbb{1}\{\cdot, \cdot\}$  is  $\frac{1}{\sigma\sqrt{2\pi}}$ -Lipschitz continuous with respect to its  
1258 both components, and (b) is derived from condition 3.1. For the term (23), we can apply the same  
1259 method to derive its upper bound:  
1260

$$\begin{aligned} 1261 & \left| \mathbb{E} [\tilde{\mathbb{1}} \{ \phi(Y, z_{\theta_0}(X)) \leq r_{\theta_0}(X) \}] - \mathbb{E} [\tilde{\mathbb{1}} \{ \phi(Y, z_\theta(X)) \leq r_\theta(X) \}] \right| \\ 1262 & \leq \mathbb{E} [\left| \tilde{\mathbb{1}} \{ \phi(Y, z_{\theta_0}(X)) \leq r_{\theta_0}(X) \} - \tilde{\mathbb{1}} \{ \phi(Y, z_\theta(X)) \leq r_\theta(X) \} \right|] \\ 1263 & \leq \frac{1}{\sqrt{2\pi}\sigma} \mathbb{E} [|\phi(Y, z_\theta(X)) - \phi(Y, z_{\theta_0}(X))| + |r_\theta(X) - r_{\theta_0}(X)|] \\ 1264 & \leq \frac{(L_z L_\phi + L_r)\epsilon}{\sqrt{2\pi}\sigma}. \\ 1265 \end{aligned}$$

1266 For term (22), by Hoeffding's inequality and a union bound over  $\theta_0 \in \Theta_\epsilon$ , with probability at least  
1267  $1 - \delta$ ,  
1268

$$\begin{aligned} 1269 & \sup_{\theta_0 \in \Theta_\epsilon} \left| \frac{1}{n} \sum_{i=1}^n \tilde{\mathbb{1}} \{ \phi(Y_i, z_{\theta_0}(X_i)) \leq r_{\theta_0}(X_i) \} - \mathbb{E} [\tilde{\mathbb{1}} \{ \phi(Y, z_{\theta_0}(X)) \leq r_{\theta_0}(X) \}] \right| \\ 1270 & \leq \sqrt{\frac{\log(2\mathcal{N}(\Theta, \|\cdot\|_\infty, \epsilon)) + \log(1/\delta)}{2n}}. \\ 1271 \end{aligned}$$

1272 Combining these bounds yields:  
1273

$$\mathbb{E} [\tilde{\mathbb{1}} \{ \phi(Y, z_\theta(X)) \leq r_\theta(X) \} \mid \mathcal{D}_n] \geq 1 - \alpha - \sqrt{\frac{\log(2\mathcal{N}(\Theta, \|\cdot\|_\infty, \epsilon)) + \log(1/\delta)}{2n}} - \frac{2(L_z L_\phi + L_r)\epsilon}{\sqrt{2\pi}\sigma}$$

1274 with probability at least  $1 - \delta$ . Finally, we quantify the discrepancy between the robustness  
1275  $\mathbb{E} [\mathbb{1}\{\phi(Y, z_\theta(X)) \leq r_\theta(X)\}]$  and its smoothed version  $\mathbb{E} [\tilde{\mathbb{1}}\{\phi(Y, z_\theta(X)) \leq r_\theta(X)\}]$ . Let  $f_\theta(\cdot)$   
1276

1296 denote the density of  $V_\theta(X, Y)$ . Then:

$$\begin{aligned}
 & \mathbb{E} [|\mathbb{1}\{\phi(Y, z_\theta(X)) \leq r_\theta(X)\} - \mathbb{1}\{\phi(Y, z_\theta(X)) \leq r_\theta(X)\}|] \\
 &= \int_{-\infty}^0 \left(1 - \frac{1}{2} \left(1 + \text{erf}\left(\frac{-t}{\sqrt{2}\sigma}\right)\right)\right) f_\theta(t) dt + \int_0^{+\infty} \frac{1}{2} \left(1 + \text{erf}\left(\frac{-t}{\sqrt{2}\sigma}\right)\right) f_\theta(t) dt \\
 &\stackrel{(a)}{\leq} \frac{\rho_0}{2} \int_{-\infty}^0 1 - \text{erf}\left(\frac{-t}{\sqrt{2}\sigma}\right) dt + \frac{\rho_0}{2} \int_0^{+\infty} 1 + \text{erf}\left(\frac{-t}{\sqrt{2}\sigma}\right) dt \\
 &\stackrel{(b)}{\leq} \sqrt{\frac{\pi}{2}} \sigma \rho_0,
 \end{aligned}$$

1306 where (a) follows from the bounded density assumption 3.2, and (b) is derived via standard Gaussian  
1307 integral identities. Incorporating this bound into the previous result, we conclude that with  
1308 probability at least  $1 - \delta$ ,

$$\begin{aligned}
 \mathbb{P}\{\phi(Y, z_{\hat{\theta}}(X)) \leq r_{\hat{\theta}}(X) \mid \mathcal{D}_n\} &\geq 1 - \alpha - \sqrt{\frac{\log(2\mathcal{N}(\Theta, \|\cdot\|_\infty, \epsilon)) + \log(1/\delta)}{2n}} \\
 &\quad - \frac{2(L_z L_\phi + L_r)\epsilon}{\sqrt{2\pi}\sigma} - \sqrt{\frac{\pi}{2}} \sigma \rho_0.
 \end{aligned}$$

□

1316 The key difference from the non-smoothed case is the presence of the term  $\sqrt{\frac{\pi}{2}} \sigma \rho_0$ , which quantifies  
1317 the bias introduced by the smoothing. Below, we directly present the relevant optimality theorem,  
1318 as its proof and conclusions are almost identical to the non-smoothed case.

1319 **Theorem D.4 (Optimality).** *Let  $\theta_{\Delta_n}^*$  be the optimal solution of problem (5) at the robustness level*

1320  $1 - \alpha + \Delta_n$  *where  $\Delta_n = \sqrt{\frac{\log(2\mathcal{N}(\Theta, \|\cdot\|_\infty, \epsilon)) + \log(1/\delta)}{2n}} + \frac{2(L_z L_\phi + L_r)\epsilon}{\sqrt{2\pi}\sigma} + \sqrt{\frac{\pi}{2}} \sigma \rho_0$ . Under the same*  
1321 *conditions of Theorem 3.3, conditioning on  $\mathcal{D}_n$ , we have*

$$\mathbb{E} [r_\theta(X) - r_{\theta_{\Delta_n}^*}(X) \mid \mathcal{D}_n] \leq 4B_r \sqrt{\frac{\log(2\mathcal{N}(\Theta, \|\cdot\|_\infty, \epsilon)) + \log(1/\delta)}{2n}} + \frac{4L_r}{n},$$

1326 with probability at least  $1 - 2\delta$ .

## 1328 E EXPERIMENTAL DETAILS AND ADDITIONAL RESULTS

### 1330 E.1 EXPERIMENTAL DETAILS OF CRC

1332 To accelerate the alternating optimization of CRC and promote stable convergence, we partition the  
1333 labeled data into two mutually exclusive parts: the first part is used for pretraining CRC, with the  
1334 resulting parameters serving as initialization for subsequent alternating optimization; the second part  
1335 is exclusively dedicated to the alternating optimization phase.

1336 The baseline method employs the same partitioning strategy: the first portion trains the prediction  
1337 model, while the second portion is used for calibration or solving downstream optimization tasks.  
1338 To ensure comparability, all methods uniformly employ the same scoring function and optimization  
1339 objective in experiments.

1340 **Pre-training** Pre-training of the CRC can be approached in two ways depending on the shape  
1341 of the prediction set: For ellipsoidal prediction sets, the neural network outputs the parameters  
1342 of a multivariate Gaussian, namely the mean vector  $\hat{\mu}(\cdot)$  and the covariance matrix  $\hat{\Sigma}(\cdot)$ . We  
1343 parameterize  $\hat{\Sigma}(\cdot)$  via a Cholesky factorization,  $\hat{\Sigma}(\cdot) = L(\cdot)L(\cdot)^\top$ , where  $L(\cdot)$  is lower triangular.  
1344 To guarantee positive definiteness, we add a small diagonal jitter to the predicted covariance, i.e.,  
1345  $\Sigma' = \Sigma + \epsilon I$  which raises the eigenvalue floor and ensures numerical stability of the Cholesky factor-  
1346 ization. Additionally, our training objective is to maximize the Gaussian log-likelihood, equivalently  
1347 to minimize the negative log-likelihood:

$$\mathcal{L}_\theta = \frac{1}{(2\pi)^{\frac{d}{2}} |\Sigma|^{\frac{1}{2}}} \exp\left(-\frac{1}{2} (y - \mu)^\top \Sigma^{-1} (y - \mu)\right).$$

For box prediction sets, we use quantile regression to directly estimate quantiles. Concretely, we train a neural network  $f_\theta(x)$  to output the  $\alpha$ -level quantile for input  $x$ . The  $1 - \alpha$  confidence interval is constructed as  $[f_\theta^{\alpha/2}(x), f_\theta^{1-\alpha/2}(x)]$ . Benefiting from quantile regression, our training objective is to minimize pinball loss. Given a quantile level  $\alpha \in (0, 1)$  and prediction  $\hat{y} = f_\theta(x)$ , the loss for target  $y$  is

$$\mathcal{L}_\alpha(y, \hat{y}) = \begin{cases} \alpha(y - \hat{y}), & \text{if } y > \hat{y}, \\ (1 - \alpha)(\hat{y} - y), & \text{if } y \leq \hat{y}. \end{cases}$$

**Optimization** For CRC optimization, we use the `cvxpylayers` (Agrawal et al., 2019) Python package to implement the implicit function differentiation. The optimization is performed using the Adam optimizer, and we select the optimal combination of learning rates ( $1e-2, 1e-3, 1e-4$ ) and L2 weight decay values ( $0, 1e-2, 1e-3$ ) to minimize the optimization loss. **Moreover, to mitigate overfitting and ineffective training, 20% of the data used for optimization is held out as a validation set. Early stopping is triggered when the loss on the validation set fails to decrease for 10 consecutive iterations or when the predefined maximum number of iterations is reached.**

**Smoothing parameters sensitivity** For CRC method, we approximate the indicator with a smooth surrogate  $\mathbb{1}\{a \leq b\} = \frac{1}{2}(1 + \text{erf}(\frac{b-a}{\sqrt{2}\sigma}))$ . We compared the sensitivity of different smoothing parameters  $\sigma$  on CRC. The experimental results are summarized in Table 2.

Table 2: The results of different smoothing parameters sensitivity of CRC at the nominal level  $\alpha = 0.1$ , where the sample size is  $n = 1500$ . The prediction sets are ellipsoids.

Method	Smoothing parameter $\sigma$	Risk Certificate	Decision Loss	Robustness (%)	Coverage (%)
CRC-E	0.01	$8.678 \pm 0.299$	$7.072 \pm 0.220$	$89.8 \pm 0.7$	$60.8 \pm 5.6$
	0.05	$8.633 \pm 0.295$	$7.070 \pm 0.219$	$89.9 \pm 0.6$	$59.6 \pm 5.5$
	0.10	$8.641 \pm 0.306$	$7.071 \pm 0.221$	$90.3 \pm 0.5$	$59.4 \pm 5.7$
	0.15	$8.643 \pm 0.315$	$7.070 \pm 0.221$	$90.5 \pm 0.6$	$59.6 \pm 5.7$
	0.20	$8.649 \pm 0.308$	$7.070 \pm 0.220$	$90.2 \pm 0.5$	$59.6 \pm 5.7$

**Lagrange multiplier update schedule sensitivity** For dual variable  $\lambda$ , we investigated the results of CRC on Lagrange multiplier update schedule sensitivity which refers to the number of model parameter optimization steps performed before each update of  $\lambda$ . The experimental results will be shown in Table 3.

Table 3: The results of lagrange multiplier update schedule of CRC at the nominal level  $\alpha = 0.1$ , where the sample size is  $n = 1500$ . The prediction sets are ellipsoids.

Method	$\lambda$ update schedule	Risk Certificate	Decision Loss	Robustness (%)	Coverage (%)
CRC-E	1	$8.641 \pm 0.334$	$7.109 \pm 0.251$	$89.9 \pm 0.5$	$58.7 \pm 5.8$
	2	$8.528 \pm 0.302$	$7.106 \pm 0.251$	$90.4 \pm 0.6$	$56.4 \pm 5.5$
	4	$8.478 \pm 0.278$	$7.105 \pm 0.251$	$90.1 \pm 0.5$	$55.4 \pm 4.8$
	8	$8.452 \pm 0.282$	$7.105 \pm 0.251$	$89.7 \pm 0.6$	$55.2 \pm 4.9$

## E.2 BASELINE METHODS

**CRO** The CRO method is our implementation of the Predict-then-Calibrate framework proposed by Sun et al. (2023). Specifically, we first train a predictive model to parameterize the uncertainty set (e.g., outputting the mean and covariance of ellipsoidal prediction sets). Subsequently, we construct a prediction set on the calibration set that satisfies the target coverage requirement. Finally, the prediction set is directly embedded into a downstream robust optimization problem to solve for decisions and minimize task loss. Thus, this method reduces task loss while enhancing solution stability, all while ensuring coverage.

**E2E** E2E is an end-to-end robust optimization method proposed by Chenreddy & Delage (2024) and Yeh et al. (2024). Unlike CRO, E2E aims to bridge uncertainty calibration with downstream task objectives by minimizing target loss through global optimization. Specifically, E2E first trains a prediction model capable of outputting parameters of uncertainty sets. It then computes non-conformity scores on the calibration set, determines the threshold  $q$  that satisfies the nominal coverage  $1 - \alpha$ , and constructs the uncertainty set accordingly. Finally, under this uncertainty set, the robust optimization problem is solved to obtain the current task loss. The gradients of the task loss with respect to model parameters are backpropagated through the differentiable optimization layer to the prediction model, enabling collaborative updates of model parameters and task objectives. Consequently, the model achieves better alignment with real-world decisions while ensuring coverage and reducing task loss. For a fair comparison, we set the loss function in E2E method as the expected risk certificate.

### E.3 DENSITY PLOT OF SIMULATION IN SECTION 5.1

The density plots of the risk certificate of three methods are given in Figure 6. Compared with other baseline methods, CRC has achieved the best performance.

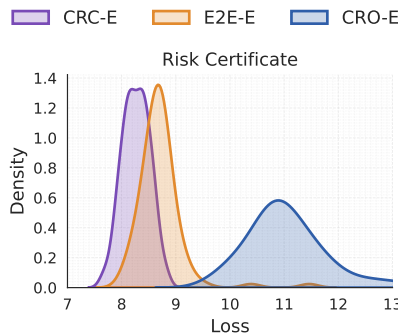


Figure 6: The densities of risk certificate on synthetic data when  $\alpha = 0.15$  and  $n = 1500$ .

### E.4 COMPARISON RESULTS OF RAC AND CRC

Based on the RA-CPO/RA-DPO framework, Kiyani et al. (2025) proposed the Risk-Averse Calibration (RAC) method to solve decision-making problems in classification settings. However, this method strictly relies on the finiteness of the label space and the decision space, i.e.,  $|\mathcal{Y}| < \infty, |\mathcal{Z}| < \infty$ . Consequently, the RAC method is more suitable for classification problems and is not applicable to regression problems since constructing the prediction set in Kiyani et al. (2025) requires solving the Value-at-Risk optimization problem, which is generally not tractable when the space is continuous. In contrast, our method is grounded in the CRO framework and derives final decisions by directly optimizing over the space of prediction sets, thereby maintaining applicability to continuous decision spaces.

To evaluate the performance of the RAC and CRC methods in regression tasks, we have to make certain adjustments to the RAC method. Specifically, a simple regression problem can be converted into a classification problem via discretization—that is, by partitioning the response and decision space into discrete bins, thus allowing RAC to be applied. However, it is important to note that in general regression settings involving high-dimensional response (such as the 15-dimensional U.S. stock problem in Section 5.2), discretization often leads to substantial computational overhead and considerable information loss, making the application of RAC infeasible. To ensure the validity of the RAC method, we consider the following simple regression problem with loss function  $\phi(y, z) = -y^\top z$  and decision space  $\mathcal{Z} = \{z \in [0, 1]^2 : \|z\|_1 = 1\}$ . The data is generated by

$$Y_1 = -1.33 \cdot \epsilon_1$$

$$Y_2 = -1 + 0.5 \cdot \epsilon_2$$

where  $Y = (Y_1, Y_2) \in \mathbb{R}^2$ , and  $\epsilon = (\epsilon_1, \epsilon_2) \in \mathbb{R}^2$ . The covariate  $X \sim N(0, I_2)$  is the spurious feature and noise  $\epsilon_1, \epsilon_2$  are independent standard Gaussian random variables. When implementing the RAC method, we need to discretize both the decision space and the label space as follows.

1458  
 1459  
 1460  
 1461  
 1462  
 1463  
 1464  
 1465

- For the decision space  $\mathcal{Z}$ , we divide the first dimension  $z_1 \in [0, 1]$  into  $J$  equally-spaced points  $\{z_{1,1}, \dots, z_{1,J}\}$ . Due to the constraint  $z_1 + z_2 = 1$ , the decision space is discretized into the finite set  $\mathcal{Z}_{\text{dis}} = \{(z_{1,1}, 1 - z_{1,1}), \dots, (z_{1,J}, 1 - z_{1,J})\}$ .
- For the label space  $\mathcal{Y}$ , we first restrict each dimension of  $Y$  to the interval between its 1% and 99% quantiles. This creates a bounded two-dimensional box, which benefits the RAC method by ensuring a bounded loss. This box is then divided uniformly into  $L \times L$  regions, and the discretized label space  $\mathcal{Y}_{\text{dis}}$  is composed of the top-right endpoints of these regions.

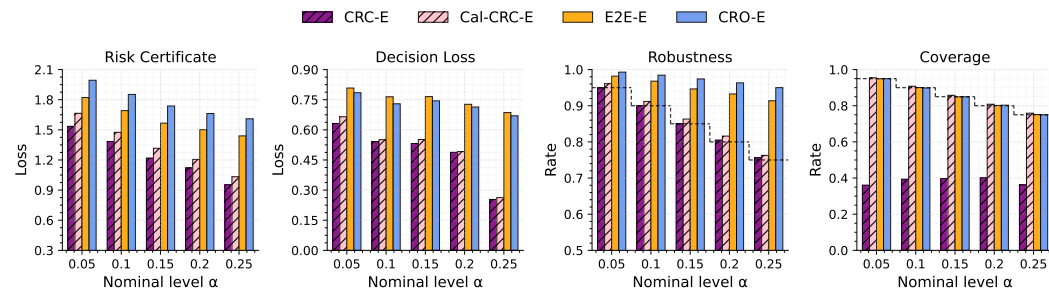
1466 The experimental results are reported in Table 4.

1467  
 1468 Table 4: The simulation results of CRC and RAC at the nominal level  $\alpha = 0.1$ , where the sample  
 1469 size is  $n = 2000$ . For the abbreviation  $\text{RAC}(J, L)$ , the numbers  $J, L$  refer to the discretization  
 1470 refinement of decision space and label space, respectively.

Method	Risk Certificate	Decision Loss	Robustness (%)	Coverage (%)
CRC-E	<b>1.384 ± 0.049</b>	<b>0.541 ± 0.065</b>	<b>90.0 ± 0.8</b>	36.1 ± 1.7
RAC(6, 2)	1.730 ± 0.039	0.803 ± 0.021	89.0 ± 1.0	89.8 ± 1.1
RAC(6, 4)	1.687 ± 0.032	0.612 ± 0.072	90.7 ± 0.9	89.9 ± 1.0
RAC(6, 8)	1.592 ± 0.038	0.725 ± 0.042	91.6 ± 0.9	89.8 ± 1.0
RAC(11, 2)	1.732 ± 0.038	0.803 ± 0.021	89.1 ± 1.0	89.8 ± 1.0
RAC(11, 4)	1.684 ± 0.033	0.576 ± 0.066	91.0 ± 0.9	89.9 ± 0.9
RAC(11, 8)	1.583 ± 0.036	0.697 ± 0.042	91.6 ± 0.9	89.9 ± 1.0

## E.5 SIMULATION RESULTS ON CAL-CRC

The experiment results of Cal-CRC under ellipsoid prediction set are shown in Figure 7, where the simulation setting is the same as that in Appendix E.4.



1496 Figure 7: The results of risk certificate, decision loss, robustness, and coverage on synthetic data  
 1497 when varying nominal level  $\alpha$  with identical sample size  $n = 2000$ . The horizontal gray dashed  
 1498 lines refer to robustness levels. The prediction sets are ellipsoids.

## E.6 SIMULATION RESULTS ON POLYHEDRAL PREDICTION SET

In this section, we adopt the methodology from Bärmann et al. (2016) to construct a parametric formulation for polyhedral prediction sets and integrate it into our proposed CRC framework. Simulation experiments demonstrate that under polyhedral prediction sets, our method still exhibits better performance compared to baseline approaches.

Following Bärmann et al. (2016), the derivation of a parametric form for polyhedral prediction sets is inspired by the parametric representation of ellipsoidal prediction sets. Let  $\mathbb{B}^q = \{y \in \mathbb{R}^q : \|y\|_2 \leq 1\}$  denote the unit sphere in  $\mathbb{R}^q$ , and let  $\mu_\theta(\cdot) : \mathbb{R}^p \rightarrow \mathbb{R}^q$  and  $\Sigma_\theta(\cdot) : \mathbb{R}^p \rightarrow \mathbb{R}^{q \times q}$  represent the parameterized mean and covariance functions with parameters  $\theta$ , respectively. The parametric ellipsoidal prediction set can be equivalently defined as:

$$\mathcal{U}_\theta^E(x) = \left\{ y \in \mathbb{R}^q : \Sigma_\theta^{-1/2}(x)(y - \mu_\theta(x)) \in \mathbb{B}^q \right\}.$$

1512 Now, let  $\mathcal{B}^q$  be a polyhedral outer  $\epsilon$ -approximation of  $\mathbb{B}^q$ , defined by  
 1513

$$1514 \quad \mathcal{B}^q = \{y : Ky \leq k\}, \quad (24)$$

1515 where  $K \in \mathbb{R}^{m \times q}$ ,  $k \in \mathbb{R}^m$  are a fixed matrix and vector, respectively, and  $m$  denotes the number  
 1516 of polyhedral facets. The corresponding parametric polyhedral prediction set is then given by:  
 1517

$$1518 \quad \mathcal{U}_\theta^P(x) = \left\{ y \in \mathbb{R}^q : \Sigma_\theta^{-1/2}(x)(y - \mu(x)) \in \mathcal{B}^q \right\} \\ 1519 \\ 1520 \quad = \left\{ y \in \mathbb{R}^q : K\Sigma_\theta^{-1/2}(x)y \leq k + K\Sigma_\theta^{-1/2}(x)\mu_\theta(x) \right\}. \quad (25)$$

1522 The construction of  $\mathcal{B}^q$  depends on the dimension  $q$  and the approximation tolerance  $\epsilon$ . For instance,  
 1523 when  $q = 2$  and  $\epsilon = 0.01$ , an  $m = 23$ -facet polyhedron ensures that the approximation error remains  
 1524 below  $\epsilon$ . In this case, the components in (24) are specified as:  
 1525

$$1526 \quad k = \mathbf{1}_{23}, \quad K = \begin{bmatrix} a_1 \\ a_2 \\ \vdots \\ a_{23} \end{bmatrix} \text{ where } a_i = \left[ \cos\left(\frac{2\pi i}{23}\right), \sin\left(\frac{2\pi i}{23}\right) \right] \text{ for } i = 1, \dots, 23.$$

1531 The polyhedral prediction set  $\mathcal{U}_\theta^P$  can be directly incorporated into the CRC framework. For example,  
 1532 in a portfolio optimization problem with loss function  $\phi(y, z) = -y^\top z$  and decision space  $\mathcal{Z} =$   
 1533  $\{z : z \in [0, 1]^q : \|z\|_1 = 1, z \geq 0\}$ . We can establish that both the decision  $z_\theta(x)$  and the risk  
 1534 certificate  $r_\theta(x)$  are differentiable with respect to  $\theta$ . This enables the search of optimal prediction  
 1535 sets via gradient-based optimization. Furthermore, the theoretical conditions outlined in Section 3.3  
 1536 continue to hold, ensuring the validity of the corresponding theorems in this extended setting.

1537 In this simulation, we compared the performance of CRC with other methods. The experimental  
 1538 setup remains consistent with that described in Appendix E.4. The experimental results are summa-  
 1539 rized in Table 5.

1540  
 1541 Table 5: The simulation results under polyhedral prediction set with nominal level  $\alpha = 0.1$ , where  
 1542 the sample size is  $n = 2000$ .

Method	Risk Certificate	Decision Loss	Robustness (%)	Coverage (%)
CRC-P	<b>1.493</b> $\pm 0.067$	<b>0.852</b> $\pm 0.037$	<b>90.3</b> $\pm 0.5$	$23.5 \pm 1.8$
CRO-P	$1.844 \pm 0.028$	$0.978 \pm 0.012$	$95.9 \pm 0.6$	$90.1 \pm 0.9$
E2E-P	$1.689 \pm 0.024$	$0.954 \pm 0.026$	$93.3 \pm 0.9$	$89.9 \pm 0.9$

## 1550 E.7 ABLATION EXPERIMENTAL RESULTS ON CRC 1551

1552 In this section, we conducted ablation experiments on CRC to compare the performance of CRC and  
 1553 calibrated method. For CRC, we used the parameters of the pre-trained model as the initial values  
 1554 for iteration. For Cal-CRC, we calibrated the model after CRC optimization. For Cal method,  
 1555 we calibrated the pre-trained model. The experimental setup is the same as Section 5.1 and the  
 1556 experimental results are summarized in Table 6.

1557  
 1558 Table 6: The results of CRC ablation experiments with nominal level  $\alpha = 0.1$ , where the sample  
 1559 size is  $n = 1500$ . The prediction sets are ellipsoids.

Method	Risk Certificate	Decision Loss	Robustness (%)	Coverage (%)
CRC-E	<b>8.660</b> $\pm 0.561$	$7.053 \pm 0.465$	$89.5 \pm 0.8$	$59.8 \pm 5.9$
Cal-CRC-E	$9.413 \pm 0.516$	$7.108 \pm 0.469$	<b>90.9</b> $\pm 1.1$	<b>90.5</b> $\pm 1.2$
Cal-E	$9.581 \pm 0.589$	$7.081 \pm 0.462$	$93.5 \pm 1.3$	$93.2 \pm 1.4$